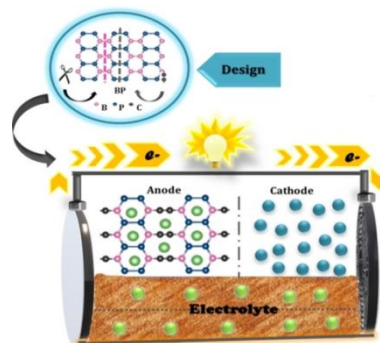


Sl. No.	<p style="text-align: center;"><b>IIT Ropar</b>  <b>List of Recent Publications with Abstract</b>  <b>Coverage: March, 2023</b></p>
1.	<p><a href="#">A data-driven passive islanding detection scheme</a>  MV Reddy, S De, R Sodhi - IEEE 10th Power India International Conference (PIICON), 2023</p> <p><b>Abstract:</b> This paper proposes a novel statistical parameters based data driven approach for passive islanding detection. The proposed scheme relies in the voltage data, measured at the point of common coupling, and is comprised of three stages. The Stage-1 quickly detects what is termed as coarse islanding, Stage-2 computes the decaying DC detector (DDCD), and 3) finally, the digital relay logic (DRL) is devised in Stage-3. The proposed scheme is tested as per the IEEE-1547, UL 1741 and IEC-62116 standards. Various tests are investigated on the modified IEEE-13 bus system, modeled in PSCAD/EMTDC, under stringent test scenarios such as power mismatch, induction motor starting effect, capacitor bank switching and various level of loads changes, considered for both single and multiple DG systems. The test results reveal that the proposed scheme can detect islanding in less than 2 cycles, and results in nearly zero non detection zone (NDZ). Also, the scheme can very well be used for single-phase microgrids too as it relies only on the single phase voltage information.</p>
2.	<p><a href="#">A heterogeneous stacking ensemble-based security framework for detecting phishing attacks</a>  B Subba - National Conference on Communications, 2023</p> <p><b>Abstract:</b> This paper proposes a heterogeneous stacking ensemble-based security framework comprising three different base-level classifiers, and a single meta-level classifier for detecting phishing attacks. The proposed framework initially extracts 24 different URL based and 20 distinct web-page based feature from a given URL corpus. These features are then used to create feature vectors for training the base-level classifiers of the proposed framework. The trained base-level classifiers are then evaluated on the unseen feature vectors from the test set. The output vectors produced by the trained base-level classifiers are then combined into a dataframe object, and used for training and evaluating a fully connected neural network(FCNN) based meta-level classifier. The trained meta-level classifier makes the final prediction about whether the web-pages corresponding to given URLs are benign or malicious(phishing). Experimental results on two benchmark datasets namely, PhishTank &amp; UNB datasets show that the proposed framework achieves an accuracy of 99% on the binary class PhishTank &amp; UNB datasets, while it achieves an accuracy of 98% on multiclass UNB dataset. The proposed framework is also shown to outperform other similar phishing attack detection frameworks proposed in the literature.</p>
3.	<p><a href="#">A lightweight deep residual attention network for single image super resolution</a>  Inderjeet, JS Sahambi - National Conference on Communications, 2023</p> <p><b>Abstract:</b> In this paper, sparse coding has been used in learning-based single image super-resolution (SR) for text images to improve the accuracy of optical character recognition (OCR). For single image SR, we create a data-driven model with deep residual attention. The deep residual attention algorithm is built on a new deep architecture that has a high representational capability. In the proposed method the architecture consists of a residual network and a dual attention network. The feature recalibration is achieved by using Channel Attention and Spatial attention technique. The proposed model uses a residual map to recover lost high-frequency features and aids in overcoming the lower spatial resolution issue. Extensive testing on the Set5, Set14, BSD100, and Urban100 datasets shows that DRA is more effective and efficient for single image SR than other reported techniques. The experiments show encouraging results for optical character recognition (OCR) application.</p>
4.	<p><a href="#">A review of image fusion: Methods, applications and performance metrics</a>  S Singh, H Singh, G Bueno, O Deniz, S Singh... - Digital Signal Processing, 2023</p>

	<p><b>Abstract:</b> The same sensor or a number of image sensors are used to take a series of photographs in order to gather as much data as possible about the scene. Several imaging techniques are used to retrieve entire information from the source under observation. Image fusion (IF) is used to create a new image that incorporates comprehensive information from many photographs. The various images may be captured from different viewpoints, different imaging sensors i.e., visible (VIS) and IR camera, different modalities i.e., computed tomography (CT) and magnetic resonance image (MRI), hyper spectral images i.e., panchromatic and multi-spectral satellite images, multi-exposure images and multi-focus images. Owing to the growing mandates and development of image enhancement schemes, numerous fusion methods were recently formulated. Consequentially, we are doing a survey study to document the methodological development in IF techniques. The outline of picture merging technologies is described in this article. Ultimately, latest state-of-the-art fusion techniques are also demonstrated. Readers will gain insights on current discoveries and their implications for the future through a review of diverse image fusion in various areas and fusion quality metrics.</p>
5.	<p><a href="#">A standardized extract of coleus forskohlii root protects rats from ovariectomy-induced loss of bone mass and strength, and impaired bone material by osteogenic and anti-resorptive mechanisms</a>  C Kulkarni, S Sharma...N Kumar... - <i>Frontiers in Endocrinology</i>, 2023</p> <p><b>Abstract:</b>  Introduction: In obese humans, Coleus forskohlii root extract (CF) protects against weight gain owing to the presence of forskolin, an adenylate cyclase (AC) activator. As AC increases intracellular cyclic adenosine monophosphate (cAMP) levels in osteoblasts that has an osteogenic effect, we thus tested the skeletal effects of a standardized CF (CFE) in rats.  Methods: Concentrations of forskolin and isoforskolin were measured in CFE by HPLC. CFE and forskolin (the most abundant compound present in CFE) were studied for their osteogenic efficacy in vitro by alkaline phosphatase (ALP), cAMP and cyclic guanosine monophosphate (cGMP) assays. Femur osteotomy model was used to determine the osteogenic dose of CFE. In growing rats, CFE was tested for its osteogenic effect in intact bone. In adult ovariectomized (OVX) rats, we assessed the effect of CFE on bone mass, strength and material. The effect of forskolin was assessed in vivo by measuring the expression of osteogenic genes in the calvarium of rat pups.  Results: Forskolin content in CFE was 20.969%. CFE increased osteoblast differentiation and intracellular cAMP and cGMP levels in rat calvarial osteoblasts. At 25 mg/kg (half of human equivalent dose), CFE significantly enhanced calcein deposition at the osteotomy site. In growing rats, CFE promoted modeling-directed bone formation. In OVX rats, CFE maintained bone mass and microarchitecture to the level of sham-operated rats. Moreover, surface-referent bone formation in CFE treated rats was significantly increased over the OVX group and was comparable with the sham group. CFE also increased the pro-collagen type-I N-terminal propeptide: cross-linked C-telopeptide of type-I collagen (PINP : CTX-1) ratio over the OVX rats, and maintained it to the sham level. CFE treatment decreased the OVX-induced increases in the carbonate-to-phosphate, and carbonate-to-amide-I ratios. CFE also prevented the OVX-mediated decrease in mineral crystallinity. Nanoindentation parameters, including modulus and hardness, were decreased by OVX but CFE maintained these to the sham levels. Forskolin stimulated ALP, cAMP and cGMP in vitro and upregulated osteogenic genes in vivo.  Conclusion: CFE, likely due to the presence of forskolin displayed a bone-conserving effect via osteogenic and anti-resorptive mechanisms resulting in the maintenance of bone mass, microarchitecture, material, and strength.</p>
6.	<p><a href="#">Acetylene-mediated borophosphene dirac materials as efficient anode materials for lithium-ion batteries</a>  K Esackraj, NVR Nulakani, VSK Choutipalli... - <i>ChemPhysChem</i>, 2023</p>

**Abstract:** Generally, graphynes have been generated by the insertion of acetylenic content ( $-C\equiv C-$ ) in the graphene network in different ratios. Also, several aesthetically pleasing architectures of two-dimensional (2D) flatlands have been reported with the incorporation of acetylenic linkers between the heteroatomic constituents. Prompted by the experimental realization of boron phosphide, which has provided new insights on the boron-pnictogen family, we have modelled novel forms of acetylene-mediated borophosphene nanosheets by joining the orthorhombic borophosphene stripes with different widths and with different atomic constituents using acetylenic linkers. Structural stabilities and properties of these novel forms have been assessed using first-principles calculations. Investigation of electronic band structure elucidates that all the novel forms show the linear band crossing closer to the Fermi level at Dirac point with distorted Dirac cones. The linearity in the hole and electronic bands impose the high Fermi velocity to the charge carriers close to that of graphene. Finally, we have also unravelled the propitious features of acetylene-mediated borophosphene nanosheets as anodes in Li-ion batteries.

**Graphical Abstract:** The acy-BP nanosheets are structurally stable and coupled with anisotropic mechanical properties and Dirac electronic properties. They are potential candidates for Li-ion battery anodes with optimal binding energies, diffusion barriers and open circuit voltage.



[Aerial image dehazing with attentive deformable transformers](#)

A Kulkarni, S Murala - IEEE/CVF Winter Conference on Applications of Computer Vision (WACV), 2023

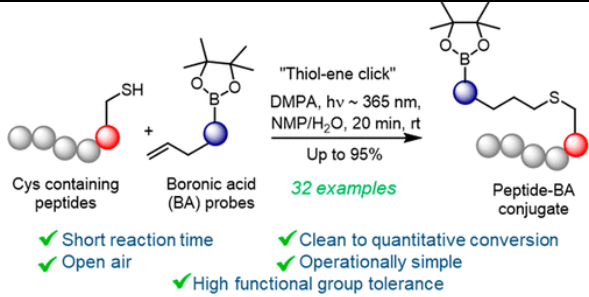
7.

**Abstract:** Aerial imagery is widely utilized in visual data dependent applications such as military surveillance, earthquake assessment, etc. For these applications, minute texture in the aerial image are essential as any disturbance can cause inaccurate prediction. However, atmospheric haze severely reduces the visibility of the scene to be analysed, and hence takes a toll on accuracy of higher level applications. Existing methods either utilize additional prior while training, or produce sub-optimal outputs on different densities of haze degradation, due to absence of local and global dependencies in the extracted features. Therefore, it is essential to have a texture preserving algorithm for aerial image dehazing. In light of this, we propose a work that introduces a novel deformable multi-head attention with spatially attentive offset extraction based solution for aerial image dehazing. Here, the deformable multi-head attention is introduced to reconstruct fine level texture in the restored image. We also introduce spatially attentive offset extractor in the deformable convolution for focusing on relevant contextual information. Further, edge boosting skip connections are proposed for effectively passing edge features from shallow layers to deeper layers of the network. Thorough experimentation on synthetic as well as real-world data, along with extensive ablation study, demonstrate that the proposed method outperforms the prevailing works on aerial image dehazing. The code is provided at <https://github.com/AshutoshKulkarni4998/AIDTransformer>.

8.	<p><a href="#">An artificial neural network surrogate model for repeater optimization in the presence of parametric uncertainty for hybrid copper-graphene interconnect networks</a>  A Sharif, S Pathania, S Kushwaha, S Roy, R Sharma, BK Kaushik - IEEE MTT-S International Conference on Numerical Electromagnetic and Multiphysics Modeling and Optimization (NEMO), 2023</p> <p><b>Abstract:</b> In this paper, an artificial neural network model is developed to predict the statistics of the optimal number and size of repeaters required to minimize the power delay product (PDP) of on-chip hybrid copper-graphene interconnect networks when subject to parametric uncertainty. The proposed ANN model is a composite of two smaller ANN models. One ANN model is used to emulate the per-unit-length parameters of the interconnects as functions of the geometrical, physical, and material parameters of the network. A second ANN model takes as inputs the outputs of the first ANN model and predicts the corresponding optimal number and size of the repeaters required in the network. Overall, the composite ANN model enables the use of analytic expressions instead of expensive and repeated full-wave electromagnetic (EM) simulations to solve the repeater optimization problem. This composite ANN model is used in a Monte Carlo framework for efficient statistical analysis.</p>
9.	<p><a href="#">Analytical method for optimal control of switched reluctance generator</a>  G Kumawat, V Shah, S Payami - IEEE 10th Power India International Conference (PIICON), 2023</p> <p><b>Abstract:</b> This paper presents an analytical method to optimally calculate the turn-on angles for the switched reluctance generator (SRG) interfaced with a bidirectional DC-DC converter (BDDC). The proposed analytical method considers the nonlinear inductance profile of the SRG drive and the back electromotive force (BEMF) developed, which are usually neglected with the classical analytical methods. The proposed method automatically adjusts the excitation parameters concerning the operating speed. Thus, the proposed method calculates the excitation angle, which mainly depends upon prime mover speed, dc-link voltage, reference current and the slope of the non-linear inductance profile of SRG. So when the speed increases, the optimal turn-on excitation angle is online, varying with speed to ensure the proper initial excitation of SRG. The prototype 4-phase SRG is designed in ANSYS/Maxwell, and the SRG model obtained is then developed in MATLAB/Simulink environment. The claims of the proposed analytical method are verified via simulation and experimental validation.</p>
10.	<p><a href="#">Analyzing the behavioural changes of various fluvial geomorphological parameters using multi-temporal satellite images for the Godavari River, India</a>  T Prashanth, S Ganguly – Copernicus Meetings: Conference Proceedings, 2023</p> <p><b>Abstract:</b> Fluvial geomorphology is the study of various landforms while analyzing the changes that are happening on the earth surface due to climate change and anthropogenic activities. Fluvial geomorphological parameters change due to natural processes like erosion, transportation, and deposition of sediments. It also changes due to manmade activities such as the construction of dams, canals, irrigation projects, etc. In this regard, the present study aims to analyze the changes in various fluvial geomorphological parameters of the Godavari River basin such as sinuosity index, braiding index, channel length index, channel count index, etc. using the Landsat images at a frequency of every 2 years from 2000 to 2022, along the length of the channel in the Godavari River, India. The second objective of this study is to perform a river bank stability analysis by using the Automatic Water Extraction Index (AWEI) at different time scales. Thirdly, we aim to quantify length, areal and relief parameters using ALOS PALSAR Digital Elevation Model (DEM) for different sub-basins of the Godavari. Due to the changes in the geomorphology, cross-section of the river is altered; the silt content increases near the hydraulic structures, the velocity of the water changes, the sinuosity (meandering) increases and it tends to the formation of oxbow lakes. This analysis helps to investigate the performance of</p>

	<p>the sub-basins of Godavari River and how much sensitive they are to erosion. An economical river bank stabilization technique can be suggested based on the rate of river bank shift and type of soil information obtained from Food and Agricultural Organization.</p>
11.	<p><a href="#">Asymptotically accurate analytical solution for timoshenko-like deformation of functionally graded beams</a>  Amandeep, SJ Singh, SS Padhee - Journal of Applied Mechanics, 2023</p> <p><b>Abstract:</b> A closed-form analytical solution is developed for a planar inhomogeneous beam subjected to transverse loading, using Variational Asymptotic Method (VAM). The VAM decouples the problem into a cross-sectional and an along-the-length analysis, leading to a set of ordinary differential equations. These equations along with associated boundary conditions have been solved to obtain the closed-form analytical solutions. Three distinct gradation models have been used to validate the present formulation against 3D FEA and few prominent results from the literature. Excellent agreement has been obtained for all the test cases. Key contributions of the present work are (a) the solutions have been obtained without any ad-hoc and a-prior assumptions (b) the ordered warping solutions results in Euler-Bernoulli type deformation in the zeroth-order, whereas the higher-order solutions provide novel closed-form expressions for transverse shear strain and stress. Finally, the effect of inhomogeneity on various field variables has been analyzed and discussed.</p>
12.	<p><a href="#">Biological knowledge capture and representation inspired by zachman framework principles</a>  S Sharma, P Sarkar - International Journal on Interactive Design and Manufacturing, 2023</p> <p><b>Abstract:</b> The International Journal on Interactive Design and Manufacturing (IJIDeM) presents interdisciplinary research, technical issues, and original industrial implementations. It examines the development, handling, and design of highly realistic, multi-sensorial virtual prototypes for improving decision-making in product design and manufacturing. Readers discover cutting-edge research in the fields of mechatronics, design and manufacturing sciences, numerical and mechanical engineering, and virtual reality.</p>
13.	<p><a href="#">Chamoli flash floods of 7th February, 2021 and recent deformation: A PSInSAR and deep learning neural network (DLNN) based perspective</a>  A Tripathi, M Moniruzzaman, AR Reshi, K Malik, RK Tiwari... - Natural Hazards Research, 2023</p> <p><b>Abstract:</b> The 7th of February 2021, Joshimath flood scenario was one such event that caused widespread damage and led to complete washout of the many hydroelectric power projects located on the course of Dhauliganga River. The physical monitoring and mapping of such events is a difficult task that often involves deployment of labour force in inhospitable terrains. Therefore, remote sensing techniques are used for the mapping and machine learning model-based predictions for future scenarios. Synthetic Aperture RADAR (SAR) remote sensing has been widely used over the years for accurate estimation of many natural and anthropogenic disaster events. This study utilizes Persistent Scatterer SAR interferometry (PSInSAR) technique to map the surface displacement of the 2021 flood scenario and make predictions for future displacement using a Deep Learning Neural Network (DLNN) model. 16 images of both ascending and descending pass were taken for the estimation of Line of Sight (LOS) displacement velocity mapping between January 2020 and April 2021 for Tapovan area. Further, 36 images from January 2020 to November 2022, in ascending and descending passes were used for prediction of future LOS surface displacement using a DLNN model for Joshimath town to see the possible impact of February 7, 2021 event. The PSInSAR LOS displacements were found to be <math>-1.2</math> cm–<math>1.2</math> cm between January 1, 2020 and April 16, 2021, for Tapovan region where the floods had occurred on February 7, 2021. The predicted LOS displacement was observed to be <math>-10</math> cm–<math>10</math> cm for December 2022 for Joshimath town. These observations clearly indicate the impact of the event to Joshimath town and as one of the causative factors of recent</p>

	observations of widespread cracks in the buildings in the region.
14.	<p><a href="#">Convective heat transfer enhancement using impingement jets in channels and tubes: A comprehensive review</a> R Kumar, R Nadda... - Alexandria Engineering Journal, 2023</p> <p><b>Abstract:</b> The industries utilize fluid heating and cooling in various applications such as production, power generation, electronics, and transportation. Many techniques have been applied / proposed to efficiently convert solar energy into thermal energy. These enhancements techniques include employing corrugated absorber plate, adding extended surfaces to the upper or lower channels, integrating artificial roughness on heated plate, jet impingement on plate and use of energy storage medium. Jet impingement is a well-known method which enhances the amount of heat that is transferred convectively from the working fluid to the absorber plate. The study of the heat transfer process employing diverse geometrical jet configurations, which are of relevance in a wide range of engineering applications, is still lacking despite the enormous number of jet impingement studies. The present study rigorously analyzed the previous works to provide essential information regarding crucial roughened geometries and geometric parameters for optimum heat transfer enhancement. This is very crucial information/aid for technical people and researchers working in the field, performance improvement of solar air heaters. The precise information related to flow parameters and heat transfer can be used by researcher in their future work which save the time as well as cost of experimental set up. The current review research's goal is to analyze and assess the systems and technologies that are already in use and those that will likely be developed in the future. If decision-makers and practitioners wish to choose the most cutting-edge and inventive technologies for heat transfer enhancement, this article may help to provide guidance. As a result, the findings of this review article may be very beneficial to distinct energy sector stakeholders.</p>
15.	<p><a href="#">Crisis and contagion in cryptocurrency market</a> B Garg, K Rai, R Pachoriya, M Thappa - Buletin Ekonomi Moneter dan Perbankan, 2023</p> <p><b>Abstract:</b> The paper examines whether an unanticipated event like the COVID-19 crisis has strengthened the contagion in the cryptocurrency market utilizing samples of data representing the pre-crisis and post-crisis periods. Employing the wavelet coherence and DCC-GARCH(1,1) models, we identify that the cryptocurrency market started integrating from 2018 as volatility within the market reduced. Our main finding is that the cryptocurrency market is highly interconnected and that the contagion strengthened during the crisis period. We draw appropriate policy implications from these findings.</p>
16.	<p><a href="#">Cysteine-selective installation of functionally diverse boronic acid probes on peptides</a> S Chatterjee, A Bandyopadhyay - Organic Letters, 2023</p> <p><b>Abstract:</b> The current methods for direct late-stage and residue-selective installation of a versatile boronic acid (BA) repertoire on peptides are inadequate for a wide range of applications. Here, we show the suitability and efficiency of thiol-ene radical click chemistry to install functionally versatile BA derivatives on numerous bioactive, native peptides. Our work highlights that the methodology is operationally simple and adaptable for applications with BA-modified peptides, such as cyclization, conjugation, and functional group alteration.</p>

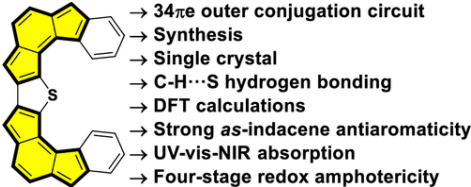
	
17.	<p><a href="#">Decoherence and entropy generation in an open quantum scalar-fermion system with Yukawa interaction</a>  S Bhattacharya, N Joshi, S Kaushal - <i>The European Physical Journal C</i>, 2023</p> <p><b>Abstract:</b> We have studied the decoherence mechanism in a fermion and scalar quantum field theory with the Yukawa interaction in the Minkowski spacetime, using the non-equilibrium effective field theory formalism appropriate for open systems. The scalar field is treated as the system whereas the fermions as the environment. As the simplest realistic scenario, we assume that an observer measures only the Gaussian 2-point correlator for the scalar field. The cause of decoherence and the subsequent entropy generation is the ignorance of information stored in higher-order correlators, Gaussian and non-Gaussian, of the system and the surrounding. Using the 2-loop 2-particle irreducible effective action, we construct the renormalised Kadanoff–Baym equation, i.e., the equation of motion satisfied by the 2-point correlators in the Schwinger–Keldysh formalism. These equations contain the non-local self-energy corrections. We then compute the statistical propagator in terms of the 2-point functions. Using the relationship of the statistical propagator with the phase space area, we next compute the von Neumann entropy, as a measure of the decoherence or effective loss of information for the system. We have obtained the variation of the entropy with respect to various relevant parameters. We also discuss the qualitative similarities and differences of our results with the scenario when both the system and the environment are scalar fields.</p>
18.	<p><a href="#">Design flood estimation for ungauged catchments in krishna river basin using a transformation-based approach to regional flood frequency analysis</a>  A Singh, S Chavan – <i>Copernicus Meetings: Conference Proceedings</i>, 2023</p> <p><b>Abstract:</b> Estimation of flood quantiles at ungauged sites is a vital aspect of the design and planning of hydraulic structures. There are various approaches such as Conventional Index Flood (CIF), Logarithmic Index Flood (LIF), and Population Index Flood (PIF), etc, that have been established to evaluate flood quantile at ungauged sites. These conventional approaches assume that the scale and shape parameters of frequency distributions remain identical for all the sites in a homogeneous region. However, this assumption may not be valid for hydrologically similar real-world catchments. Recently, a transformation-based mathematical approach to regional frequency analysis was proposed by Basu and Srinivas (2013), which ensured the assumption of having identical scale and shape parameters across the sites in a hydrologically similar homogeneous region. The approach involves (i) identification of appropriate frequency distribution representing the homogeneous region, (ii) Mapping the flood quantile (corresponding to various non-exceedance probability) from the original space to a dimensionless space, where values of parameters of distributions at sites in the region remain identical, (iii) construction of regional growth curve in dimensionless space and, (iv) Mapping of dimensionless regional growth curve to original space by applying inverse transformation equations. This study presents an application of the approach given by Basu and Srinivas (2013) for estimating the design flood estimate at ungauged catchments in the Krishna river basin. The delineation of hydrologically similar regions is performed by using a global <i>k</i>-means clustering algorithm. In this study, The parameters of the inverse transformation equations are obtained by</p>

	<p>using log-linear regression model (LLRM), generalized additive model (GAM), and multivariate adaptive regression spline (MARS). Finally, a comparative analysis is performed to assess the efficacy of the regression models in estimating the parameters of transformation equations. The result revealed that the Regional Flood Frequency Analysis (RFFA) using Basu and Srinivas's (2013) approach is effective for reliable prediction of design flood estimates in Indian watersheds.</p>
19.	<p><a href="#">Determination of joint roughness coefficient using a cost-effective photogrammetry technique</a> S Rohilla, R Sebastian - <i>Bulletin of Engineering Geology and the Environment</i>, 2023</p> <p><b>Abstract:</b> The presence of discontinuities in the rock mass is extremely crucial in many engineering applications of rock mechanics. The estimation of the joint roughness coefficient (JRC) utilising easily accessible camera-friendly devices and application software has recently gained prominence. The joint roughness coefficient of a jointed rough surface may be calculated using either contact methods (physically contacting the surface to get the profile) or non-contact methods (extraction of the profile without physically touching the surface using laser profilometry or 3D laser scanning and photogrammetry techniques). The 3D laser scanner is widely used for its accuracy in obtaining the surface topography of rock masses; however, the practice is often uneconomical due to the high equipment cost. In this study, the smartphone photogrammetry technology is used to extract the three-dimensional surface topography of a jointed rough surface in order to evaluate the JRC. For the comparative study, the surface profile was retrieved using a surface profilometer, 3D scanner and photogrammetry method. The JRC values for the surface profiles gathered through smartphone photogrammetry, 3D scanning and surface profilometer have been estimated using visual analysis, fractal dimension and statistical techniques. The study found that the surface profile generated using the photogrammetric approach utilising smartphone delivers more realistic profiling than the surface profilometer because of the lower least count and greater precision. The predicted JRC values for smartphone photogrammetry profiles agreed well with the JRC values obtained for 3D scanner and surface profilometer profiles.</p>
20.	<p><a href="#">Determination of the relative orientation between <math>^{15}\text{N}</math>-<math>^1\text{H}</math> dipolar coupling and <math>^1\text{H}</math> chemical shift anisotropy tensors under fast MAS solid-state NMR</a> N Sehrawat, E Nehra, KK Rohilla, T Kobayashi...MK Pandey - <i>Journal of Magnetic Resonance</i>, 2023</p> <p><b>Abstract:</b> In this work, we have proposed a proton-detected three-dimensional (3D) <math>^{15}\text{N}</math>-<math>^1\text{H}</math> dipolar coupling (DIP)/<math>^1\text{H}</math> chemical shift anisotropy (CSA)/<math>^1\text{H}</math> chemical shift (CS) correlation experiment to measure the relative orientation between the <math>^{15}\text{N}</math>-<math>^1\text{H}</math> dipolar coupling and the <math>^1\text{H}</math> CSA tensors under fast magic angle spinning (MAS) solid-state NMR. In the 3D correlation experiment, the <math>^{15}\text{N}</math>-<math>^1\text{H}</math> dipolar coupling and <math>^1\text{H}</math> CSA tensors are recoupled using our recently developed windowless <math>C</math>-symmetry-based <math>C31/3</math>-ROCSA (recoupling of chemical shift anisotropy) DIPSHIFT and <math>C31/3</math>-ROCSA pulse-based methods, respectively. The 2D <math>^{15}\text{N}</math>-<math>^1\text{H}</math> DIP/<math>^1\text{H}</math> CSA powder lineshapes extracted using the proposed 3D correlation method are shown to be sensitive to the sign and asymmetry of the <math>^1\text{H}</math> CSA tensor, a feature that allows the determination of the relative orientation between the two correlating tensors with improved accuracy. The experimental method developed in this study is demonstrated on a powdered U-<math>^{15}\text{N}</math> L-Histidine.HCl·H<sub>2</sub>O sample.</p>
21.	<p><a href="#">Development and analysis of moments preserving finite volume schemes for multi-variate nonlinear breakage model</a> A Das, J Paul, S Heinrich, J Kumar – <i>Proceedings of the Royal Society A</i>, 2023</p> <p><b>Abstract:</b> Modelling and simulation of collisional particle breakage mechanisms are crucial in several physical phenomena (asteroid belts, molecular clouds, raindrop distribution etc.) and process industries (chemical, pharmaceutical, material etc.). This paper deals with the</p>



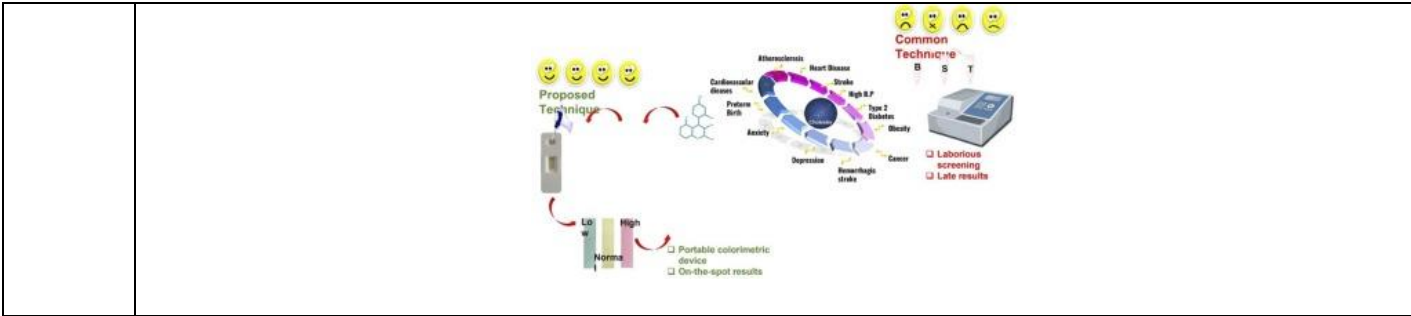
	<p>development and analysis of schemes to numerically solve the multi-dimensional nonlinear collisional fragmentation model. Two numerical techniques are presented based on the finite volume discretization method. It is shown that the proposed schemes are consistent with the hypervolume conservation property. Moreover, the number preservation property law also holds for one of them. Detailed mathematical discussions are presented to establish the convergence analysis and consistency of the multi-dimensional schemes under predefined restrictions on the kernel and initial data. The proposed schemes are shown to be second-order convergent. Finally, several numerical computations (one-, two- and three-dimensional fragmentation) are performed to validate the numerical schemes.</p>
22.	<p><a href="#">Diagnosis of Interturn Short-Circuits in SRMs by High-Frequency Switching of Phases Amid Low-Torque Unaligned Rotor Positions</a>  M Alam, S Payami - IEEE Transactions on Industrial Electronics, 2023</p> <p><b>Abstract:</b> The inherent problems of torque ripple, noise, and vibrations associated with switched reluctance motors (SRMs) are escalated when the machine is subjected to interturn short-circuits (ITSCs). Also, leaving it unchecked can ultimately lead to a complete winding short-circuit due to the insulation failure owing to the heat produced by locally generated hotspots. To avoid such ruinous damage, the diagnosis of ITSCs is very critical. This article proposes a method of diagnosing ITSCs by injecting high-frequency signals in the phases in their low-torque regions around unaligned rotor positions. The proposed method utilizes the drive power converter to inject and diagnose the ITSCs and, thus, requires no additional hardware. It has a higher sensitivity even toward minor fault conditions, i.e., as low as ITSC of four turns (<math>\approx 4\%</math> ITSC over a phase). The devised fault indicator is immune to load or speed variation and, hence, better detection reliability. Also, the method can diagnose the fault under load and speed transients, proving it to be more robust. Experiments are performed on a test rig of customized 8/6 SRM emulating the ITSCs to verify the potency of the proposed scheme.</p>
23.	<p><a href="#">Digital screening and brief intervention for alcohol misuse in college students: A pilot, mixed-methods, cluster randomized controlled trial from a low-resourced setting</a>  A Ghosh, NC Krishnan, S Kathirvel, RR Pillai, D Basu...A Kumar - Asia-Pacific Psychiatry, 2023</p> <p><b>Abstract:</b>  Introduction  We examined the feasibility and acceptability of digital screening and brief intervention (d-SBI) for alcohol misuse in college students; the effectiveness of d-SBI was our secondary outcome. We also explored the barriers and facilitators of d-SBI.  Methods  The study design is a mixed-methods, pilot, and cluster randomized trial. Five colleges from a northern city in India were randomly allocated to d-SBI and control groups. One hundred and ninety-one students were screened, and 25 (male = 23 and female = 2) participants (age <math>19.62 \pm 2.58</math> years) fulfilled eligibility. All participants completed follow-up assessments at 3 months. In-depth interviews were done with 11 participants. Alcohol Use Disorder Identification Test (AUDIT) based screening brief intervention was provided on a web portal- or mobile application in the d-SBI group. The control group received digital screening and brief education. Direct questions and usage statistics assessed the measurement acceptability of the intervention. We compared the change in AUDIT scores in the intervention groups over 3 months post-intervention. Thematic analyses of transcripts of interviews were done by inductive coding.  Results  Most participants reported that d-SBI was user-friendly (80%), advice was appropriate (80%), and perceived it to be useful (72%). Ninety-six percent of users, who logged in, completed screening. There was a significant decrease in AUDIT scores both in d-SBI (<math>p &lt; .001</math>) and control groups (<math>p &lt; .001</math>). Time and group significantly affected the mean AUDIT score, but</p>

	<p>time × group interaction was non-significant. Thematic analysis revealed six overarching themes.</p> <p>Conclusions</p> <p>Digital SBI for alcohol misuse is acceptable, feasible, and possibly effective among college students from low-resource settings.</p>
24.	<p><a href="#">Dinitrogen reduction coupled with methanol oxidation for low overpotential electrochemical NH<sub>3</sub> synthesis over cobalt pyrophosphate as bifunctional catalyst</a> D Gupta, A Kafle, TC Nagaiah - Small, 2023</p> <p><b>Abstract:</b> Electrochemical dinitrogen (N<sub>2</sub>) reduction to ammonia (NH<sub>3</sub>) coupled with methanol electro-oxidation is presented in the current work. Here, methanol oxidation reaction (MOR) is proposed as an alternative anode reaction to oxygen evolution reaction (OER) to accomplish electrons-induced reduction of N<sub>2</sub> to NH<sub>3</sub> at cathode and oxidation of methanol at anode in alkaline media thereby reducing the overall cell voltage for ammonia production. Cobalt pyrophosphate micro-flowers assembled by nanosheets are synthesized via a surfactant-assisted sonochemical approach. By virtue of structural and morphological advantages, the maximum Faradaic efficiency of 43.37% and NH<sub>3</sub> yield rate of 159.6 μg h<sup>-1</sup> mg<sub>ca</sub><sup>-1</sup> is achieved at a potential of -0.2 V versus RHE. The proposed catalyst is shown to also exhibit a very high activity (100 mA mg<sup>-1</sup> at 1.48 V), durability (2 h) and production of value-added formic acid at anode (2.78 μmol h<sup>-1</sup> mg<sub>cat</sub><sup>-1</sup> and F.E. of 59.2%). The overall NH<sub>3</sub> synthesis is achieved at a reduced cell voltage of 1.6 V (200 mV less than NRR-OER coupled NH<sub>3</sub> synthesis) when OER at anode is replaced with MOR and a high NH<sub>3</sub> yield rate of 95.2 μg h<sup>-1</sup> mg<sub>cat</sub><sup>-1</sup> and HCOOH formation rate of 2.53 μmol h<sup>-1</sup> mg<sup>-1</sup> are witnessed under full-cell conditions.</p>
25.	<p><a href="#">Dissipation of incident wave energy by two floating horizontal porous plates over a trench type bottom</a> S Choudhary, SC Martha - Ships and Offshore Structures, 2023</p> <p><b>Abstract:</b> This work investigates the scattering of oblique incident waves by two floating horizontal porous plates over a trench-type sea bed to study the role of different pairs of barriers in dissipating the incident wave energy. This problem is modelled based on Darcy's law for flow past a porous structure. Havelock's expansions of water wave potentials, suitable matching conditions, and the algebraic least-square method handle the boundary value problem. The role of the horizontal porous plates is studied by analysing the scattering coefficients, energy loss, hydrodynamic wave force and free surface elevation through graphs which show a periodic oscillatory pattern as a function of gap length. The study reveals that if the porous effect parameter of plates or the length of plates is increased, more energy is dissipated and the plates experience less wave force, and the free surface elevation on the lee side is decreased. The present results also signify that as compared to rigid plates, significant changes are found in wave scattering coefficients, hydrodynamic force and free surface elevation due to the consideration of one porous plate along with one rigid plate and also two porous plates, where a pair of porous plates are more effective as compared to one porous plate. The present study reveals that the scattering of water waves by two floating horizontal porous plates over uneven bottom topography plays a vital role in constructing floating structures having more staying power in harsh wave environments.</p>
26.	<p><a href="#">Does bank competition affect the transmission mechanism of monetary policy through bank lending channel? Evidence from India</a> B Rakshit, S Bardhan - Journal of Asian Economics, 2023</p> <p><b>Abstract:</b> This paper empirically investigates how intensified competition in the Indian banking affects the transmission of monetary policy through bank lending channel over the period 1997–2017. Additionally, this study examines the impact of deposit and loan market channels on bank's credit growth. Results obtained through two-step system-GMM reveal that a higher degree of market power weakens the monetary policy transmission mechanism for the entire</p>

	<p>banking industry and across ownerships. Results show that higher market power in the deposit and loan markets weakens the impact of monetary policy on bank loan supply. The findings of this study extend important policy measures that can strengthen the transmission mechanism of monetary policy by reducing the adverse effects of changes in bank competition.</p>
27.	<p><a href="#">Dominating antiaromatic character of <i>as</i>-indacene decides overall properties of a formally aromatic dicyclopenta[<i>c</i>]fluorenothiophene</a>  PK Sharma, D Mallick, H Sharma, S Das - <i>Organic Letters</i>, 2023</p> <p><b>Abstract:</b> Dicyclopenta[<i>c</i>]fluorenothiophene <b>5</b> was synthesized as the isoelectronic polycyclic heteroarene analogue of an <i>as</i>-indacenodifluorene with a <math>(4n + 2)\pi</math>-electron perimeter. Single-crystal and <math>^1\text{H}</math> NMR analyses indicated a quinoidal ground state for <b>5</b>, which was supported by theoretical calculations while suggesting a degree of antiaromaticity of the <i>as</i>-indacene subunit greater than that for <i>s</i>-indacenodifluorene <b>3</b>. The dominant antiaromaticity for <b>5</b> was evidenced by the broad weakly intense absorption tail reaching the near-IR region, four-stage redox amphotericity, and small HOMO–LUMO energy gap.</p> <div style="text-align: center;">  <p>→ 34<math>\pi</math>e outer conjugation circuit  → Synthesis  → Single crystal  → C–H<math>\cdots</math>S hydrogen bonding  → DFT calculations  → Strong <i>as</i>-indacene antiaromaticity  → UV-vis-NIR absorption  → Four-stage redox amphotericity</p> </div>
28.	<p><a href="#">Dynamics of co-current gas–liquid film flow through a slippery channel featured</a>  R Vellingiri - <i>Physics of Fluids</i>, 2023</p> <p><b>Abstract:</b> We consider a thin liquid film in a wide inclined channel being driven by gravity and co-current turbulent gas flow. The bottom plate with which the liquid is in contact with is taken to be slippery, and we impose the classic Navier slip condition at this substrate. Such a setting finds application in technological processes as well as nature (e.g., distillation, absorption, and cooling devices). The gas–liquid problem can be decoupled by making certain reasonable assumptions. Under these assumptions, we solve the gas problem to obtain the tangential and normal stresses acting at the wavy gas–liquid interface for arbitrary waviness. In modeling the liquid layer dynamics, we make use of the stresses computed in the gas problem as inputs to the interface boundary conditions. We develop the long-wave model and the weighted-integral boundary layer (WIBL) model to describe the thin film dynamics. We perform a linear stability of these reduced order models to scrutinize the effect of wall slip, liquid flow rate, and the gas shear on the stability of the flat film solution. It is found that the wall slip promotes the instability of the flat interface. Furthermore, we compute solitary wave solutions of the WIBL model by implementing Keller's pseudo-arc length algorithm on a periodic domain. We observe that the wave speed as well as the wave amplitude are attenuated on incrementing the liquid slip at the substrate. We corroborate these findings with the time-dependent computations of the nonlinear WIBL model.</p>
29.	<p><a href="#">Efficient algorithms for fair clustering with a new notion of fairness</a>  S Gupta, G Ghalme, NC Krishnan, S Jain - <i>Data Mining and Knowledge Discovery</i>, 2023</p> <p><b>Abstract:</b> We revisit the problem of fair clustering, first introduced by Chierichetti et al. (Fair clustering through fairlets, 2017), which requires each protected attribute to have approximately equal representation in every cluster, i.e., a Balance property. Existing solutions to fair clustering are either not scalable or do not achieve an optimal trade-off between clustering objectives and fairness. In this paper, we propose a new notion of fairness which we call <math>\tau</math>-ratio fairness, that strictly generalizes the Balance property and enables a fine-grained efficiency vs. fairness trade-off. Furthermore, we show that a simple greedy round-robin-based algorithm achieves this trade-</p>

	<p>off efficiently. Under a more general setting of multi-valued protected attributes, we rigorously analyze the theoretical properties of the proposed algorithm, the Fair Round-Robin Algorithm for Clustering Over-End (FRACO<sub>EF</sub>). We also propose a heuristic algorithm, Fair Round-Robin Algorithm for Clustering (FRAC), that applies round-robin allocation at each iteration of a vanilla clustering algorithm. Our experimental results suggest that both FRAC and FRACO<sub>EF</sub> outperform all the state-of-the-art algorithms and work exceptionally well even for a large number of clusters.</p>
30.	<p><a href="#">Extending merge resolution to a family of qbf-proof systems</a>  S Chede, A Shukla - <i>International Symposium on Theoretical Aspects of Computer Science, 2023</i></p> <p><b>Abstract:</b> Merge Resolution (MRes [Olaf Beyersdorff et al., 2021]) is a recently introduced proof system for false QBFs. Unlike other known QBF proof systems, it builds winning strategies for the universal player (countermodels) within the proofs as merge maps. Merge maps are deterministic branching programs in which isomorphism checking is efficient, as a result MRes is a polynomial time verifiable proof system.</p> <p>In this paper, we introduce a family of proof systems MRes-<math>\mathcal{R}</math> in which the information of countermodels are stored in any pre-fixed complete representation <math>\mathcal{R}</math>. Hence, corresponding to each possible complete representation <math>\mathcal{R}</math>, we have a sound and refutationally complete QBF-proof system in MRes-<math>\mathcal{R}</math>. To handle these arbitrary representations, we introduce consistency checking rules in MRes-<math>\mathcal{R}</math> instead of the isomorphism checking in MRes. As a result these proof systems are not polynomial time verifiable (Non-P). Consequently, the paper shows that using merge maps is too restrictive and with a slight change in rules, it can be replaced with arbitrary representations leading to several interesting proof systems.</p> <p>We relate these new systems with the implicit proof system from the algorithm in [Joshua Blinkhorn et al., 2021], which was designed to solve DQBFs (Dependency QBFs) using clause-strategy pairs like MRes. We use the OBDD (Ordered Binary Decision Diagrams) representation suggested in [Joshua Blinkhorn et al., 2021] and deduce that "Ordered" versions of the proof systems in MRes-<math>\mathcal{R}</math> are indeed polynomial time verifiable.</p> <p>On the lower bound side, we lift the lower bound result of regular MRes ([Olaf Beyersdorff et al., 2020]) by showing that the completion principle formulas (CR<sub>n</sub>) from [Mikolás Janota and João Marques-Silva, 2015] which are shown to be hard for regular MRes in [Olaf Beyersdorff et al., 2020], are also hard for any regular proof system in MRes-<math>\mathcal{R}</math>. Thereby, the paper lifts the lower bound of regular MRes to an entire class of proof systems, which use various complete representations, including those undiscovered, instead of only merge maps. Thereby proving that the hardness of CR<sub>n</sub> formulas is intact even after changing the weak isomorphism checking in MRes to the stronger consistency checking in MRes-<math>\mathcal{R}</math>.</p>
31.	<p><a href="#">Flow boiling heat transfer characteristics over horizontal smooth and microfin tubes: An empirical investigation utilizing R407c</a>  S Deb, KP Mahesh, M Das, DC Das, S Pal, R Das, AK Das - <i>International Journal of Thermal Sciences, 2023</i></p> <p><b>Abstract:</b> The flow boiling heat transfer performance of horizontal smooth and microfin tubes was investigated using the refrigerant R407c. The evaporator test tube contains an outside, inner diameter and length of 9.52, 8.52, and 1000 mm, respectively. The investigations were performed out at 283.15 and 303.15 K saturation temperatures with hot water circulation heat flux of 75 kW.m<sup>-2</sup>, refrigerant heat flux varying from 5 to 85 kW.m<sup>-2</sup>, and mass flux varied from 15 to 250 kg.m<sup>-2</sup>.s<sup>-1</sup>, keeping the area ratio of microfin tube 1.68%. The experimental results are compared to several previously recognised correlations. Experimental outcomes demonstrated that the heat transfer rate of the microfin tube is superior to the smooth tube. The percentage of heat transfer enhancement was considered to exceed in microfin tube by 28–280%. The pressure drop in regard to R407c was found to be augmented than smooth tube according to the</p>

	<p>experimental results and enhancement was achieved in microfin tube by 68–110%. Finally, a sensitivity analysis is carried out in flow boiling heat transfer phenomenon via the smooth tube.</p>
32.	<p><a href="#">Fresh evidence on the oil-stock interactions under heterogeneous market conditions</a> KB Chowdhury, B Garg - Finance Research Letters, 2023</p> <p><b>Abstract:</b> This paper ameliorates the existing empirical literature on the oil-stock nexus in three ways. First, we expand the literature on return-volatility interactions by adding non-linear dimensions to it. Second, we propose a threshold VAR asymmetric GARCH-in-mean (TVAR-AGARCH-M) model to examine the mean-spillover and return-volatility associations under heterogeneous market conditions of bull and bear markets. Third, we show that the TVAR-AGARCH-M model is superior to the benchmark VAR-GARCH-M model. Our analysis unfolds that oil price volatility affects stock returns in highly volatile market conditions but not in low-volatile states. We also find evidence of strong asymmetry wherein lagged negative shocks strongly influence volatility in oil and stock markets. Specifically, we show that countries such as Japan can benefit from hedging in international markets by diversifying their portfolio in positively correlated markets.</p>
33.	<p><a href="#">Furtherance of the material-based hydrogen storage based on theory and experiments</a> RY Sathe, TJD Kumar, R Ahuja - International Journal of Hydrogen Energy, 2023</p> <p><b>Abstract:</b> The repercussions of the burning of fossil fuels on the global air quality index need to be countered with implementable green alternatives such as the hydrogen economy. High energy density, abundance, and the eco-friendly oxidation product of hydrogen make it an ideal fossil fuel replacement. However, the quest for safe, inexpensive, and compact storage material for hydrogen remains the prime concern. The scientific community is mainly looking for two major characteristics, i.e., high hydrogen storage capacity and the onboard reversibility of the host at operable thermodynamic conditions. Since the past decade, a tremendous amount of research has been undertaken toward such material development and exploring their stable hydrogen storage characteristics. In this extensive review, we report the significant material advancements made in this decade toward the methodical and sustainable hydrogen economy. Hydrogen weight percentage (wt%), reversibility, stability, onboard feasibility, and the heat-pressure response of these prospective hydrogen storage hosts have been thoroughly discussed.</p>
34.	<p><a href="#">HgAu alloy@4H-Chromene predicated colorimetric lateral flow device: On-site rapid detection of hyper and hypocholesterolaemia</a> G Bhardwaj, R Kaur, S Saini, N Kaur, N Singh - Sensors and Actuators B: Chemical, 2023</p> <p><b>Abstract:</b> An unbalanced diet and lifestyle nowadays are very concerning as it lacks desired nutrition's which in the long term ultimately led to high cholesterol and other health problems. The present work reports the development of a HgAu alloy stabilized 4H-chromene organic nanoparticles (G4) following a simple condensation technique and characterized <i>via</i> HRTEM, SEM, AFM, DLS, EDAX, and STEM. Furthermore, G4 exhibits increased stability in comparison to bare Hg-Au alloy and ultrahigh selectivity and sensitivity towards cholesterol by changing its color from yellow to pink and blue on report of high and low levels of cholesterol respectively. The color change was quantified using RGB analysis and compared with the UV-Visible absorption data. Further for the rapid on-site detection of cholesterol, pristine paper based lateral flow device has been developed and tested for the human serum, where it gives significantly good results with a recovery percentage of 101.7% with 0.011 nM limit of detection (LOD), linearity of 99.3%, and reproducibility of <math>\pm 4\%</math> (relative standard deviation). To the best of our knowledge, the present work represents the first report on: (a) preparation of HgAu alloy@4H-chromene, and (b) detection of hypocholesterolaemia.</p> <p><b>Graphical abstract:</b></p>



35.

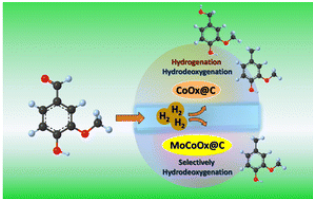
[Identification of a physiologic vasculogenic fibroblast state to achieve tissue repair](#)  
 D Pal, S Ghatak, K Singh, AS Abouhashem, M Kumar... - Nature Communications, 2023

**Abstract:** Tissue injury to skin diminishes miR-200b in dermal fibroblasts. Fibroblasts are widely reported to directly reprogram into endothelial-like cells and we hypothesized that miR-200b inhibition may cause such changes. We transfected human dermal fibroblasts with anti-miR-200b oligonucleotide, then using single cell RNA sequencing, identified emergence of a vasculogenic subset with a distinct fibroblast transcriptome and demonstrated blood vessel forming function in vivo. Anti-miR-200b delivery to murine injury sites likewise enhanced tissue perfusion, wound closure, and vasculogenic fibroblast contribution to perfused vessels in a FLII dependent manner. Vasculogenic fibroblast subset emergence was blunted in delayed healing wounds of diabetic animals but, topical tissue nanotransfection of a single anti-miR-200b oligonucleotide was sufficient to restore FLII expression, vasculogenic fibroblast emergence, tissue perfusion, and wound healing. Augmenting a physiologic tissue injury adaptive response mechanism that produces a vasculogenic fibroblast state change opens new avenues for therapeutic tissue vascularization of ischemic wounds.

36.

[Improved data fusion-based land use/land cover classification using polsar and optical remotely sensed satellite data](#)  
 A Tripathi, S Kumar, S Maithani - Spaceborne Synthetic Aperture Radar Remote Sensing: Book Chapter, 2023

**Abstract:** India today, as in most developing countries of the world, shows a rapid increase in urbanization. As there is an increased demand for land for urban expansion to cater to the migrant service population, there is also an increased demand for agricultural land for meeting the food requirements. All of this is leading to a drastic change in the land use/land cover pattern, as well as posing impacts for nature and resources more broadly. Due to their dynamic nature, urban areas can be difficult to map easily, but remote sensing is an effective tool capable of solving this problem. However, optical remote sensing has its constraints, like paucity of all-weather data; in addition, urban and fallow land areas often tend to merge since they both produce a cyan tone in a standard false colour composite (FCC) optical image. This makes their delineation and classification difficult. This study aimed to consider and utilize the different polarimetric decomposition models and to examine the backscatter based on the man-made and natural features detected in each. The multifrequency co-registered slant-range single look complex (co-SSC) of the X-band PolSAR dataset from TerraSAR-X was analysed, and various techniques, to fuse optical and PolSAR images, were compared. Out of these, the HSV (hue saturation value) fusion technique gave the best results in classification. It was found that PolSAR, due to its various modelling approaches and polarimetric combinations, has an advantage over both SAR and optical datasets and is found to minimize the ambiguity of merging urban built-up with fallow land features in the optical dataset. In this study, both quad and dual PolSAR datasets of TerraSAR-X were taken. The datasets were corrected for interior orientation angle and the speckle was removed using the refined Lee filter. Thereafter, coherent (Pauli's and Sinclair's decomposition) and incoherent decompositions (H-A- $\alpha$ , Yamaguchi, Freeman–Durden, and Van-Zyl) were applied on quad PolSAR datasets. The dual PolSAR

	<p>datasets were band rationed to generate a suitable RGB for classification. Suitable decomposition and band-rationed products were chosen based on backscatter separability for fusion with optical LISS-IV data. Based on the high spectral separability of the HSV-fused product, it was chosen for further classification using pixel- and object-based image classification. The different machine learning classification results were compared based on the relative classification accuracies achieved.</p>
37.	<p><a href="#">Improving the hydrodeoxygenation activity of vanillin and its homologous compounds by employing MoO<sub>3</sub>-incorporated Co-BTC MOF-derived MoCoO<sub>x</sub>@C</a>  AK Kar, SP Kaur, TJD Kumar, R Srivastava - Dalton Transactions, 2023</p> <p><b>Abstract:</b> Lignin-derived aryl ethers and vanillin are essential platform chemicals that fulfil the demands for renewable aromatic compounds. Herein, an efficient heterogeneous catalyst is reported for reforming vanillin <i>via</i> a selective hydrodeoxygenation route to 2-methoxy-4-methyl phenol (MMP), a precursor to medicinal, food, and petrochemical industries. A series of MoCoO<sub>x</sub>@C catalysts were synthesized by decorating the Co-BTC MOF with different contents of MoO<sub>3</sub> rods, followed by carbonization. Among these catalysts, MoCoO<sub>x</sub>@C-2 afforded ~99% vanillin conversion and ~99% MMP selectivity at 150 °C in 1.5 h in an aqueous medium. In contrast, CoO<sub>x</sub>@C afforded ~75% vanillin conversion and ~85% MMP selectivity. Detailed catalyst characterization revealed that CoO<sub>x</sub> and Co<sub>2</sub>Mo<sub>3</sub>O<sub>8</sub> were the active species contributing to the higher activity of MoCoO<sub>x</sub>@C-2. The excellent H<sub>2</sub>-adsorption characteristics and acidity of MoCoO<sub>x</sub>@C-2 were beneficial to the hydrodeoxygenation of vanillin and other homologous compounds. The DFT adsorption energy calculations suggested the favourable interactions of vanillin and vanillyl alcohol with the Co<sub>2</sub>Mo<sub>3</sub>O<sub>8</sub> sites in MoCoO<sub>x</sub>@C-2. The catalyst could be efficiently recycled 5 times, with a negligible loss in activity after the 5th cycle. These findings provide a systematic explication of the active sites of the mixed metal oxide-based MoCoO<sub>x</sub>@C-2 catalyst for the selective hydrodeoxygenation of vanillin to MMP, which is important for the academic and industrial catalysis community.</p> 
38.	<p><a href="#">Integrated converter with G2V, V2G, and DC/V2V charging capabilities for switched reluctance motor drive-train based EV application</a>  V Shah, S Payami - IEEE Transactions on Industry Applications, 2023</p> <p><b>Abstract:</b> The article proposes an integrated converter (IC) with driving, grid-to-vehicle (G2V), vehicle-to-grid (V2G), and DC/ vehicle-to-vehicle (V2V) charging capabilities for electric vehicle (EV) drive-train employing switched reluctance motor (SRM). During drive mode, the battery supplies the driving power, and the proposed IC independently controls the individual phases of the SRM. When EV is standstill/ idle, the proposed IC can charge the battery via standard AC and DC charging sockets. For charging the battery via a single-phase residential/public AC outlet, i.e., G2V charging, the proposed IC exhibits a power factor correction (PFC) charger. The reconfigured switches are bidirectional, facilitating the flow of power in both directions, i.e., G2V and V2G charging. For fast charging of the battery via DC source, which includes emerging DC grids, solar photovoltaic systems, and battery source of another EV, i.e., V2V charging, the proposed IC exhibits a four-quadrant DC-DC converter (FQDDC). For realizing the inductors of the PFC charger and FQDDC converter, the phase windings of SRM are reconfigured. Thus, the proposed IC eliminates the requirement of any</p>

	<p>additional non-integrated circuit, which reduces the total switch count. Also, proposed way of reconfiguring inductors results in a standstill rotor at appropriate rotor positions. The above-stated claims of the proposed IC are validated via experimental studies.</p>
39.	<p><a href="#">Interplay of reservoirs in a bidirectional system</a> A Gupta, B Pal, AK Gupta - <i>Physical Review E</i>, 2023</p> <p><b>Abstract:</b> Motivated by the interplay of multiple species in several real world transport processes, we propose a bidirectional totally asymmetric simple exclusion process with two finite particle reservoirs regulating the inflow of oppositely directed particles corresponding to two different species. The system's stationary characteristics, such as densities, currents, etc., are investigated using a theoretical framework based on mean-field approximation and are supported by extensive Monte Carlo simulations. The impact of individual species populations, quantified by filling factor, has been comprehensively analyzed considering both equal and unequal conditions. For the equal case, the system exhibits the spontaneous symmetry-breaking phenomena and admits both symmetric as well as asymmetric phases. Moreover, the phase diagram exhibits a different asymmetric phase and displays a nonmonotonic variation in the number of phases with respect to the filling factor. For unequal filling factors, the phase schema can display at most five phases including a phase that shows maximal current for one of the species.</p>
40.	<p><a href="#">Investigations on sheath voltage and current during short-circuited condition on a cross-bonded cable</a> A Das, CC Reddy - <i>IEEE 10th Power India International Conference (PIICON)</i>, 2023</p> <p><b>Abstract:</b> The Sheath is an eternal part of a cable, protects the insulation from moisture ingress, acts as an electrical shielding, and also a return path for load and fault current. Being grounded to at least any single point the cable sheath will always have either one of them or both types of phenomenon, the sheath voltage, and sheath current. To minimize the losses in the sheath, the cable sheath was bonded in a cross-bonded formation, with the presence of a sheath voltage limiter (SVL). The SVL protects the cable sheath from transients and faults. In the lifespan of the cable, the most unavoidable event is the occurrence of faults. In the presence of a short-circuited fault at a particular phase, the sheath of the other phase may also get affected, causing deterioration in the condition of the cable. In this paper, a comparative study of sheath voltage and sheath current during a short-circuited fault at each phase was studied for both cases, in the presence and absence of SVL, the simulation study was carried out with circuit simulating software.</p>
41.	<p><a href="#">Ionic Fe(III)-porphyrin frameworks for the one-pot synthesis of cyclic carbonates from olefins and CO<sub>2</sub></a> R Das, S Kamra, CM Nagaraja - <i>Inorganic Chemistry Frontiers</i>, 2023</p> <p><b>Abstract:</b> In this study, the rational construction of Fe<sup>III</sup>-centered porphyrin-based bifunctional ionic porous organic polymers (Fe-IPOP1/2) for a one-step, halogen-free, cascade transformation of olefins and CO<sub>2</sub> to cyclic carbonates as compared to the conventional two-step process involving epoxides is presented. The ionic polymers, Fe-IPOP1/2 showed selective and recyclable uptake of CO<sub>2</sub> with an interaction energy of 32.2/39.6 kJ mol<sup>-1</sup> signifying the stronger interaction of carbon dioxide with the frameworks. Both the polymers were found to be thermally stable up to 300 °C and exhibited promising catalytic performance in the one-step, halogen-free synthesis of cyclic carbonates under eco-friendly, cocatalyst/solvent-free, atmospheric pressure conditions. The excellent catalytic activity of Fe-IPOP1/2 for a one-pot synthesis of cyclic carbonates has been ascribed to the presence of highly exposed oxophilic Fe<sup>III</sup> sites and nucleophilic Br<sup>-</sup> anions in the polymers. Notably, this one-pot synthesis strategy was extended for the transformation of various substituted olefins to their respective carbonates in good yield and selectivity. Further, Fe-IPOP1 showed good reusability with retention of</p>



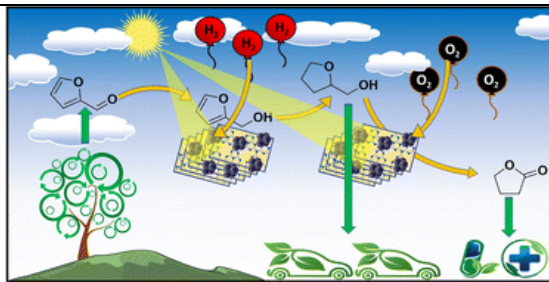
	catalytic activity for multiple cycles of usage.
42.	<p><a href="#">Joint QoS and energy-efficient resource allocation and scheduling in 5G Network Slicing</a> Saibharath S, S Mishra, C Hota - <i>Computer Communications</i>, 2023</p> <p><b>Abstract:</b> Network Slicing (NS) is fast evolving as a prominent enabler for providing tailored services in the Fifth Generation of cellular networks (5G). Network Slices are virtualized network entities formed over physical substrates, deployed for the customized application use cases. A Network Slice needs to exhibit end to end capabilities and meet Quality of Service (QoS) specifications and Service Level Agreements (SLAs). To provide end-to-end traffic management capabilities in the network slice, firstly, traffic flows are categorized into different priority traffic classes, and their severity levels are assessed. Priorities can be applied across cellular and IP based systems. Machine Learning (ML) algorithms are employed on QoS profile attributes in establishing traffic priorities in slices. Secondly, we propose a novel algorithm for NS Resource Partitioning and User Allocation. We put forward an online virtual backbone based solution for resource allocation and priority class-based packet scheduling. This joint QoS and energy efficiency driven approach is built on top of established traffic classes and dynamic power savings techniques. Finally, through Cognitive Cycles (CC), we devise better network re-configuration to obtain more energy savings. Traffic classifier modules are implemented using Jupyter notebook and Python API. Scheduling and resource allocation modules in networks slices are emulated in Mininet, Flowvisor, and Beacon and POX controllers. The simulation results reveal the reduced node consumption is achieved through the evolutionary CC algorithm, and it outperforms other standard approaches by at least 23%. Similarly, for the traffic priority prediction, from the results, we could infer Gradient Boosting and Random Forest Regressors exhibit superior accuracy with the root mean square deviation of 2.2% and 1.2% respectively when compared to other standard ML algorithms.</p>
43.	<p><a href="#">Lightweight network for video motion magnification</a> J Singh, S Murala, GSR Kosuru - <i>IEEE/CVF Winter Conference on Applications of Computer Vision (WACV)</i>, 2023</p> <p><b>Abstract:</b> Video motion magnification provides information to understand the subtle changes present in objects for applications like industrial, healthcare, sports, etc. Most state-of-the-art (SOTA) methods use hand-crafted bandpass filters, which require prior information for the motion magnification, produces ringing artifacts, and small magnification etc. While others use deep-learning based techniques for higher magnification, but their output suffers from artificially induced motion, distortions, blurriness, etc. Further, SOTA methods are computationally complex, which makes them less suitable for real-time applications. To address these problems, we proposed deep learning based simple yet effective solution for motion magnification. The proposed method uses a feature sharing and appearance encoder for better motion magnification with fewer distortions, artifacts etc. Additionally, for reducing magnification of noise and other unwanted changes, proxy-model based training is proposed. A computationally lightweight model (~0.12 M parameters) is proposed along with the base model. The performance of the proposed models is tested qualitatively and quantitatively, with the SOTA methods. Results demonstrate the effectiveness of the proposed lightweight and base model over the existing SOTA methods.</p>
44.	<p><a href="#">Multifold stiffness and fracture toughness enhancement in W-doped VO<sub>2</sub> microcrystals</a> D Verma, Y Chandran, P Uniyal, N Kumar... - <i>Journal of the American Ceramic Society</i>, 2023</p> <p><b>Abstract:</b> Vanadium dioxide is popular for the metal-insulator phase transition at 68°C. Chemical doping is one of the effective ways adopted to tune the phase transition temperature, where tungsten is known to reduce the transition temperature of VO<sub>2</sub>. This work investigates the effect of tungsten doping on the mechanical properties of VO<sub>2</sub> microcrystals and their polymer composites. Doping of VO<sub>2</sub> with W shows a systematic reduction in phase transition temperature</p>

	<p>up to 33°C for 4 wt% W-doped VO<sub>2</sub>. For 3 wt% W-doped VO<sub>2</sub>, the elastic modulus values enhance by 50%. The fracture toughness of 3 wt% W-doped VO<sub>2</sub> shows an enhancement of fourfold compared to the undoped VO<sub>2</sub>. The dynamic compressive strength of 3 wt% W-doped VO<sub>2</sub>–UHMWPE polymer composite at room temperature is found to be 7% higher than the undoped VO<sub>2</sub>–composite.</p>
45.	<p><a href="#">Multiphysics modelling and high-speed imaging-based validation of discharge plasma in micro-EDM</a>  S Raza, H Kishore, CK Nirala, KP Rajurkar - CIRP Journal of Manufacturing Science and Technology, 2023</p> <p><b>Abstract:</b> This paper describes the plasma channel formation during the micro-electrical discharge machining (micro-EDM) at various voltage and capacitance settings. A numerical model using COMSOL Multiphysics finite element is developed to estimate the plasma parameters, such as the plasma channel diameter and temperature distribution in the radial and axial directions. The numerical model also predicts the heat flux distribution responsible for material melting and subsequent removal. Additionally, the coupled numerical model explains the plasma-electrode interactions via different heat transfer mechanisms such as conduction, convection, radiation and thermionic effect. Experimental plasma diameters obtained from high-speed imaging of the discharge process were compared with the simulation results and were in close agreement, with an error between 5% and 14.5%. The simulated molten diameters at various input parameters were compared with experimental crater diameters of single craters and observed to follow a similar trend.</p>
46.	<p><a href="#">Near-infrared hyperspectral imaging for determination of protein content in barley samples using convolutional neural network</a>  T Singh, NM Garg, SRS Iyengar, V Singh - Journal of Food Measurement and Characterization, 2023</p> <p><b>Abstract:</b> The protein content is an essential quality parameter that is measured by the breeding programs and food industries to maintain high-quality standards for barley. The traditional methods for determining protein content are destructive, time-consuming, and require the use of analytical reagents and chemical solvents. Near-infrared (NIR) spectroscopy is a rapid, non-destructive technology used to predict protein content by collecting spectral information. Alternatively, near-infrared hyperspectral imaging (NIR-HSI) integrates both spatial and spectral information of the samples. In this study, spatially resolved spectral information provided by the NIR-HSI was applied to predict the protein content of the barley samples. A total of 972 barley samples (889 hulled and 83 naked barley samples) were collected, and their reference protein values were measured using an elemental analyzer. The protein content ranged from 7.4 to 14.2%, with higher values for naked barley compared to hulled barley samples. The spatial information obtained from hyperspectral imaging system was used to extract the multiple mean spectra from each sample. The spectra were pre-treated with different spectral preprocessing techniques, which were then used as inputs of convolutional neural network (CNN) and conventional predictive models. The CNN model performed better on the unprocessed spectra (herein called raw spectra) than on the preprocessed spectral data. Additionally, the end-to-end CNN model trained using multiple mean spectra extracted from each sample outperformed the conventional models. The CNN model achieved a coefficient of determination (R<sup>2</sup>) of 0.9962, root mean square error (RMSE) of 0.0823, and residual prediction deviation (RPD) of 16.15. Finally, prediction maps were used to visualize the predicted protein content of the test barley samples. The overall results support the conclusion that the CNN model established using multiple mean spectra extracted from NIR hyperspectral images of barley samples can be used to accurately predict the protein content.</p>
47.	<p><a href="#">Nested deformable multi-head attention for facial image inpainting</a>  SS Phutke, S Murala - IEEE/CVF Winter Conference on Applications of Computer Vision</p>

	<p>(WACV), 2023</p> <p><b>Abstract:</b> Extracting adequate contextual information is an important aspect of any image inpainting method. To achieve this, ample image inpainting methods are available that aim to focus on large receptive fields. Recent advancements in the deep learning field with the introduction of transformers for image inpainting paved the way toward plausible results. Stacking multiple transformer blocks in a single layer causes the architecture to become computationally complex. In this context, we propose a novel lightweight architecture with a nested deformable attention-based transformer layer for feature fusion. The nested attention helps the network to focus on long-term dependencies from encoder and decoder features. Also, multi-head attention consisting of a deformable convolution is proposed to delve into the diverse receptive fields. With the advantage of nested and deformable attention, we propose a lightweight architecture for facial image inpainting. The results comparison on Celeb HQ [25] dataset using known (NVIDIA) and unknown (QD-IMD) masks and Places2 [57] dataset with NVIDIA masks along with extensive ablation study prove the superiority of the proposed approach for image inpainting tasks. The code is available at: <a href="https://github.com/shrutiphutke/NDMA_Facial_Inpainting">https://github.com/shrutiphutke/NDMA_Facial_Inpainting</a>.</p>
48.	<p><a href="#">Non-perturbative analysis for a massless minimal quantum scalar with <math>V(\phi) = \lambda\phi^4/4! + \beta\phi^3/3!</math> in the inflationary de Sitter spacetime</a>  S Bhattacharya, N Joshi - <i>Journal of Cosmology and Astroparticle Physics</i>, 2023</p> <p><b>Abstract:</b> We consider a massless, minimally coupled quantum scalar field theory with an asymmetric self interaction, <math>V(\phi) = \lambda\phi^4/4! + \beta\phi^3/3!</math> (<math>\lambda &gt; 0</math>) in the inflationary de Sitter spacetime. The potential is bounded from below. While the <math>\beta=0</math> case has been much well studied, the motivation behind taking such a hybrid potential corresponds to the fact that it might generate finite negative vacuum expectation values of <math>V(\phi)</math> as well of <math>\phi</math>, leading to some dynamical screening of the inflationary cosmological constant <math>\Lambda</math>, at late times, with the initial conditions, <math>\langle \phi \rangle = 0 = \langle V(\phi) \rangle</math>. In this work we first compute the vacuum expectation values of <math>\phi</math>, <math>\phi^2</math> and <math>V(\phi)</math>, using the late time, non-perturbative and infrared effective stochastic formalism. The backreactions to the inflationary <math>\Lambda</math> are estimated. We also compute the dynamically generated mass of the scalar field using <math>\langle \phi^2 \rangle</math>. We next compute <math>\langle \phi^2 \rangle</math> using quantum field theory with respect to the initial Bunch-Davies vacuum at one and two loops, using the Schwinger-Keldysh formalism. These results show non-perturbative secular logarithms, growing with the cosmological time. Using next a recently proposed renormalisation group inspired formalism, we attempt to find out a resummed <math>\langle \phi^2 \rangle</math>. We have been able to resum some part of the same which contains contributions only from the local self energy. The corresponding dynamically generated mass is computed. Comparison of the stochastic and the quantum field theory results shows that they differ numerically, although they have similar qualitative behaviour. Possible reasons for such quantitative mismatch is discussed. The manifestation of strong non-classical effects in the results found via both the formalisms has been emphasised.</p>
49.	<p><a href="#">Non-uniform superlattice magnetic tunnel junctions</a>  S Chakraborti, A Sharma – <i>Nanotechnology</i>, 2023</p> <p><b>Abstract:</b> We propose a new class of non-uniform superlattice magnetic tunnel junctions (Nu-SLTJs) with the linear, Gaussian, Lorentzian, and Pöschl–Teller width and height based profiles manifesting a sizable enhancement in the TMR (<math>\approx 10^4 - 10^6\%</math>) with a significant suppression in the switching bias (<math>\approx 9</math> folds) owing to the physics of broad-band spin filtering. By exploring the negative differential resistance region in the current–voltage characteristics of the various Nu-SLTJs, we predict the Nu-SLTJs offer fastest spin transfer torque switching in the order of a few hundred picoseconds. We self-consistently employ the atomistic non-equilibrium Green's</p>

	<p>function formalism coupled with the Landau–Lifshitz–Gilbert–Slonczewski equation to evaluate the device performance of the various Nu-SLTJs. We also present the design of minimal three-barrier Nu-SLTJs having significant TMR (<math>\approx 10^4\%</math>) and large spin current for the ease of device fabrication. We hope that the class of Nu-SLTJs proposed in this work may lay the bedrock to embark on the exhilarating voyage of exploring various non-uniform superlattices for the next generation of spintronic devices.</p>
50.	<p><a href="#">On q-analogue of Euler–Stieltjes constants</a> T Chatterjee, S Garg - <i>Proceedings of the American Mathematical Society</i>, 2023</p> <p><b>Abstract:</b> Kurokawa and Wakayama [Proc. Amer. Math. Soc. 132 (2004), pp. 935–943] defined a <math>q</math>-analogue of the Euler constant and proved the irrationality of certain numbers involving <math>q</math>-Euler constant. In this paper, we improve their results and prove the linear independence result involving <math>q</math>-analogue of the Euler constant. Further, we derive the closed-form of a <math>q</math>-analogue of the <math>k</math>-th Stieltjes constant <math>\gamma_k(q)</math>. These constants are the coefficients in the Laurent series expansion of a <math>q</math>-analogue of the Riemann zeta function around <math>z=1</math>. Using a result of Nesterenko [C. R. Acad. Sci. Paris Sér. I Math. 322 (1996), pp. 909–914], we also settle down a question of Erdős regarding the arithmetic nature of the infinite series <math>\sum_{n \geq 1} \sigma_1(n)/t^n</math> for any integer <math>t &gt; 1</math>. Finally, we study the transcendence nature of some infinite series involving <math>\gamma_1(2)</math>.</p>
51.	<p><a href="#">On the prediction of particle collision behavior in coarse-grained and resolved systems</a> T De, A Das, J Kumar - <i>Particulate Science and Technology</i>, 2023</p> <p><b>Abstract:</b> The discrete element method (DEM) simulates granular processes and detects inter-particle collisions during the simulation. Detection of collision helps researchers to study the occurrence of particulate mechanisms such as aggregation, breakage, etc. DEM demands high computational costs in simulating industrial-level systems, as it involves an enormous number of particles. DEM coarse-grained model can help to overcome this high computational cost issue. However, the frequency and probability of collisions for different particle size classes may change when coarser particles are introduced. This study introduces a new mathematical formulation, namely the collision dependency function (CDF), which predicts the probability of collisions between different particle classes for systems containing resolved and coarse-grained particles. The CDF is extracted by executing one DEM simulation consisting of number-based uniformly distributed particles. Furthermore, a new optimized scheme is used inside the DEM to store the collision data efficiently. Finally, the collision probabilities between size classes obtained from DEM simulations are compared successfully against their counterparts calculated from the developed model for verification.</p>
52.	<p><a href="#">Outage analysis using probabilistic channel model for drone assisted multi-user coded cooperation system</a> P Kumar, S Bhattacharyya, S Darshi, S Majhi... - <i>IEEE Transactions on Vehicular Technology</i>, 2023</p> <p><b>Abstract:</b> This paper proposes a statistical-based channel modelling approach for a drone assisted multi-user coded cooperation (DA-MUCC) for evaluating the performance metrics of a next-generation wireless communication system. The proposed approach may find its applications in smart cities, disaster management and agriculture for building reliable communication links among ground users (GUs)/user equipments (UEs) over the scenarios where an infrastructure-based network (like a Base Station (BS)) is difficult to establish or disrupted. In such scenarios, an air-to-ground (A2G) channel is modelled based on the probabilistic approach of line-of-sight (LoS) and statistical independence of the links. The network performance of the proposed system model is evaluated by closed-form average outage probability and average rate over the Rayleigh and Rician fading channel models. The analytical performance is corroborated by Monte-Carlo simulations and also compared with the existing</p>

	<p>state-of-the-art approaches. Finally, we derive the probability density function (PDF) for signal-to-noise ratio (SNR) of relay link which is useful under the scenarios where the direct links among GUs are in the deep fade.</p>
53.	<p><a href="#">Performance analysis of porous-based taper-shaped fin for enhanced heat transfer rate using cuckoo search algorithm</a>  A Ranjan, R Das, S Pal, A Majumder, M Deb - Proceedings of the Institution of Mechanical Engineers, Part E: Journal of Process Mechanical Engineering, 2023</p> <p><b>Abstract:</b> This paper deals with the thermal and fluid flow behavior of porous and non-porous fins. Initially, a solid heat sink with circular fins is analyzed and validated. Further work is done making circular tapered porous fin of the same volume and height as of uniform circular fin. The geometrical parameters are porosity (<math>\emptyset = 0.1\text{--}0.92</math>), pore diameter (<math>d_p</math>), fiber diameter (<math>d_f</math>), radius ratio (<math>R^*</math>), and pores per inch (PPI = 10). Four different cases viz., case I (<math>R^* = 1.2</math>), case II (<math>R^* = 1.5</math>), case III (<math>R^* = 2</math>), and case IV (<math>R^* = 4</math>) of taper porous fins are considered in a computational domain with Reynolds number (<math>Re</math>) ranging 400–1900 (based upon channel inlet parameter) and air as working fluid. The Forchheimer–Brinkman extended Darcy model is considered to characterize the flow in porous media. The value of Nusselt number (<math>Nu</math>), friction factor (<math>f</math>), and thermal performance factor (TPF) is evaluated. <b>Results</b> reveal that, for case I at <math>\emptyset = 0.92</math> and PPI = 10, the value of <math>Nu</math> and TPF is approximately 63% and 159% higher than solid circular fin at <math>Re = 1876.11</math>. For case IV, the reduction in pressure drop is approximately 21.15% compared to solid circular fin at <math>Re = 1876.11</math>. For optimum <math>Nu</math>, a cuckoo search optimization is evaluated using the response surface method. Upon examination, the optimum <math>Nu</math> is obtained at the combination of <math>R^* = 1.2</math>, <math>\emptyset = 0.92</math>, and <math>Re = 1876.11</math>, which got validated against the numerical work with 0.15% accuracy.</p>
54.	<p><a href="#">Photocatalytic selective conversion of furfural to <math>\gamma</math>-butyrolactone through tetrahydrofurfuryl alcohol intermediates over Pd NP decorated g-C<sub>3</sub>N<sub>4</sub></a>  R Ghalta, R Srivastava - Sustainable Energy &amp; Fuels, 2023</p> <p><b>Abstract:</b> The photocatalytic transformation of biomass-derived platform chemicals into renewable chemicals/fuels is challenging but demanding to meet the global energy and chemical demands. Herein, a photocatalytic selective reduction strategy is reported for the selective synthesis of tetrahydrofurfuryl alcohol (THFA) from furfural (FAL) using a 150 W LED/sunlight at ambient temperature by employing 2 bar H<sub>2</sub>. Efficient light-absorbing g-C<sub>3</sub>N<sub>4</sub> was synthesized for this purpose. Different contents of Pd NPs were decorated over g-C<sub>3</sub>N<sub>4</sub> to accomplish the above transformations. 3 wt% Pd NP decorated g-C<sub>3</sub>N<sub>4</sub> exhibited nearly 100% FAL conversion and 100% THFA selectivity after 5.5 h using a 150 W white LED. THFA was transformed into <math>\gamma</math>-butyrolactone (GBL) with nearly 100% selectivity using a 150 W white LED/sunlight under ambient conditions in O<sub>2</sub> (1 bar) after 8 h. Detailed physicochemical characterization studies and optoelectronic measurements were conducted in addition to control reactions and scavenging studies to establish the structure–activity relation. Decoration of Pd NPs significantly improved the photoactivity and photoelectrochemical properties by hosting photogenerated electrons and facilitated the separation of charge carriers by improving their lifetime to participate effectively in the catalytic reactions. The catalyst exhibited efficient recyclability (measured up to five cycles) and photostability upon repetitive use. A simple, eco-friendly, reproducible, and cost-effective photocatalytic valorization of FAL to THFA and THFA to GBL would be the foundation for developing similar catalysts to produce other valuable renewable chemicals from biomass-platform chemicals.</p>



[Postmodern anxiety and the neo-victorian dialogue with the other in graham swift’s ever after](#)  
A Shekher, A Louis - English Studies, 2023

55.

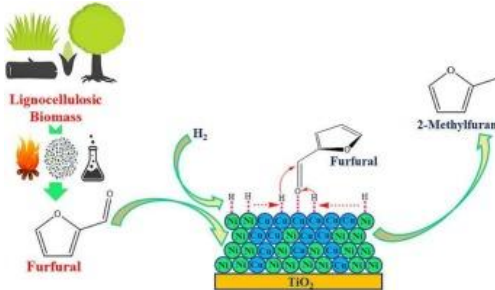
**Abstract:** Graham Swift’s *Ever After* offers a literary treatment of the existential trauma that Darwinism has brought about in the nineteenth century. Further as part of the neo-Victorian sub-genre, Swift’s work intertwines this trauma with the anxieties characterising the twentieth century present of the novel. Swift charts two journeys which ultimately fail to culminate in a “happily ever after”, due to the impact of Darwinism in one case and the struggle against postmodern existential anxiety in the other. The novel juxtaposes the predicaments of two fictional characters and renders one’s apostasy in the past as a possible means for the protagonist’s attempt to cathartically release his pent-up feelings in the present. Our essay explores how the comparative equation between the two persons belonging to different eras in the novel corresponds to Emmanuel Levinas’ conception of the “other” as a significant factor in the assertion of the “self”.

[Predicting future groundwater recharge scenario in the Punjab region of India using machine learning techniques](#)

D Banerjee, S Ganguly – Copernicus Meetings: Conference Proceedings, 2023

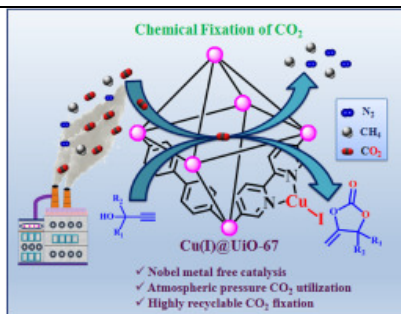
56.

**Abstract:** Over last few decades the Punjab region of India has been one of the country's leading contributors to agricultural products. The agricultural farms in the region are supplied with water from a well-established canal system and groundwater reserve in the state. The share of irrigated area in the region fed by canals and groundwater wells are 28 and 72%, respectively. The over and unscientific usage of groundwater over the years has resulted in groundwater depletion at an alarming rate. To help policymakers address the situation and develop effective plans, forecasting groundwater recharge for the future is utmost essential. The recharge process primarily governs the growth or depletion of groundwater reserve. Groundwater recharge is one of the most difficult phenomena to be quantified as it cannot be measured directly and is influenced by several processes varying spatially and temporally. Extensive research work for quantifying the groundwater recharge have been performed in the past. These investigations introduced a number of methodologies, including chemical tracers and physical procedures. These methods, however, being experimental in nature, involve significant time and investment. The use of machine learning algorithms to predict the recharge is promoted as a solution to these problems. These algorithms have proven to be efficient enough to deduce the recharge with very high accuracy. Through a variety of models, ranging from the most basic to one of the more intricate, we have attempted to forecast the recharge scenario in the Punjab region, India. Four machine learning algorithms, namely the Multi-linear regression model, Non-linear regression model (Random Forest), Multi-Layer Perceptron (MLP) and Long Short-Term Memory (LSTM) have been employed in this study. The aim was to comprehend the dependence of groundwater recharge on the factors of temperature, precipitation, soil type, LULC, and ground slope. The observed recharge for every subsequent month in a 30-year period is calculated using the observed monthly groundwater level data from observation wells located throughout Punjab. The monthly temperature and precipitation data are used for the study while soil type and ground slope for the location of the observation stations are extracted from digital elevation models

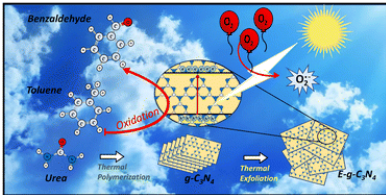
	<p>(DEMs). At intervals of three years, the LULC maps are created. The models are then used to forecast and compare with the available observation data after the entire data set was split into a training and testing set using the 80/20 method. The models were then assessed for their ability to predict observational data using the Root Mean Squared Error (RMSE) and Coefficient of Determination (<math>R^2</math>) in each case. The groundwater recharge prediction is then performed using the model with the highest accuracy.</p>
57.	<p><a href="#">Production of 2-methyl furan, a promising 2nd generation biofuel, by the vapor phase hydrodeoxygenation of biomass-derived furfural over TiO<sub>2</sub> supported Cusingle bondNi bimetallic catalysts</a>  A Jaswal, PP Singh, AK Kar, T Mondal, R Srivastava - Fuel Processing Technology, 2023</p> <p><b>Abstract:</b> This work investigates the vapor phase hydrodeoxygenation (HDO) of FFR to 2-MeF over a series of TiO<sub>2</sub>-supported mono and bimetallic Cu-Ni catalysts with a fixed Cu content (10 wt%) and varying Ni content (0–20 wt%). The catalysts were synthesized through a simple wet impregnation method, and their properties were studied in depth through an array of analytical techniques such as X-ray diffraction (XRD), H<sub>2</sub>-temperature programmed reduction (H<sub>2</sub>-TPR), Scanning Electron Microscopy (SEM), N<sub>2</sub>-physisorption, Raman spectroscopy, and NH<sub>3</sub>-temperature programmed desorption (TPD). The catalyst characterizations revealed that the addition of Ni in progressively larger amounts resulted in greater dispersion of Cu species and an increase in the surface area &amp; porosity of the bimetallic catalysts, arising from the strong interactions between NiO and CuO species. Detailed studies were carried out to evaluate the effect of various process parameters such as Ni content, temperature, and contact time on the selectivity of 2-MeF. Ni content of the bimetallic catalysts and temperature played a significant role in product distribution than the contact time. The bimetallic catalyst with the composition 10%Cu-10%Ni was observed to be the optimum, providing a FFR conversion of 100%, and a 2-MeF selectivity of 84.5% at 200 °C, H<sub>2</sub>/FFR molar ratio = 15, and WHSV = 0.87 g<sub>FFR</sub> h<sup>-1</sup> g<sub>catalyst</sub><sup>-1</sup> after 6 h time-on-stream (TOS). During the long-term catalytic activity evaluation, the catalyst exhibited a stable 100% FFR conversion and ~ 85% selectivity towards 2-MeF over a period of 12 h. Even after a period of 15 h, conversion and selectivity values remained &gt;90% and 70%, respectively.</p> <p><b>Graphical Abstract:</b></p>  <p>The graphical abstract illustrates the process of producing 2-methylfuran from biomass. It starts with 'Lignocellulosic Biomass' (represented by a tree and grass) which is converted into 'Furfural' (represented by a chemical structure). This furfural is then subjected to hydrodeoxygenation (HDO) over a 'TiO<sub>2</sub>' catalyst (represented by a grid of blue and green spheres) in the presence of 'H<sub>2</sub>'. The final product is '2-Methylfuran' (represented by its chemical structure).</p>
58.	<p><a href="#">Quantum network coding and distribution of maximally entangled states in measurement-based quantum computing</a>  C Pandey, S Gupta, RR Das, A Raina - National Conference on Communications , 2023</p> <p><b>Abstract:</b> Classical network coding uses encoding of information over networks to achieve secure and high throughput communication with low latency. Its quantum analog, namely Quantum Network Coding (QNC) is a promising protocol to achieve quantum communication over quantum networks. In this paper, we propose a method for establishing QNC in Measurement-Based Quantum Computing (MBQC), which is a universal quantum computational model. We demonstrate that the problem of multiple unicast or multiple multicast of distinct</p>

	<p>computational basis states over a quantum network can be solved by simulating existing classical networks, with the CNOT implementation in MBQC as a basis for transmitting and encoding of states. We also show how it can be further extended to simultaneously distribute the Bell pairs and Greenberger–Horne–Zeilinger (GHZ) states required for quantum communication between distant transmitter and corresponding receiver nodes of a network.</p>
59.	<p><a href="#">Rate of change of J-integral in creep-fatigue condition</a>  A Tiwari – <i>Fatigue &amp; Fracture of Engineering Materials &amp; Structures</i>, 2023</p> <p><b>Abstract:</b> The operational conditions in next generation power plants and other high temperature applications such as turbine blades in jet engines demand the component to perform under extreme conditions where metallic materials show time dependent deformation under cyclic loading conditions. Under creep-fatigue loading condition, the crack tip is exposed to both time dependent and independent plastic deformation. Conventional crack characterizing parameters such as <math>(C_t)_{avg}</math> has shown good correlation with dominant damage-based crack velocity, <math>(da/dt)_{avg}</math>. However, the true definition or prediction of crack driving forces under such scenario are vague due to limited theoretical validity of the conventional crack tip characterizing parameters, such as <math>J</math> or <math>C_t</math>. In this work, the concept of configurational forces are applied for the first time to understand the creep-fatigue crack growth behavior. The crack growth is simulated using node-release technique and the configurational forces are calculated using post processing the finite element results for calculation of <math>dJ/dt</math>.</p>
60.	<p><a href="#">Rational construction of noble metal-free Cu(I) anchored Zr-MOF for efficient fixation of CO<sub>2</sub> from dilute gas at ambient conditions</a>  A Nagaraj, R Das, CM Nagaraja - <i>Microporous and Mesoporous Materials</i>, 2023</p> <p><b>Abstract:</b> The utilization of carbon dioxide (CO<sub>2</sub>) from dilute gas as C1 feedstock for synthesis of high-value chemicals such as <math>\alpha</math>-alkylidene cyclic carbonates is one of the promising approaches towards mitigating the increasing atmospheric CO<sub>2</sub> concentration. Consequently, herein, we demonstrate the application of UiO-MOF functionalized with bipyridine sites for facile anchoring of catalytically active noble metal-free copper (I) sites by post-synthetic treatment. The Cu(I) anchored UiO-MOF exhibits an excellent catalytic activity for coupling CO<sub>2</sub> with propargylic alcohols affording <math>\alpha</math>-alkylidene cyclic carbonates, valuable commodity chemicals at mild conditions of 1 atm of CO<sub>2</sub> (balloon). Furthermore, the MOF catalyst showed good activity for fixation carbon dioxide from dilute gas (CO<sub>2</sub>:N<sub>2</sub> = 13:87%) condition. The superior catalytic performance of Cu(I)@UiO-MOF over the homogeneous counterpart has been attributed to a synergistic effect of high CO<sub>2</sub>-philicity of MOF and catalytic activity of copper (I) sites exposed in the 1D channels of the MOF. The catalyst can be recycled up to five cycles with retention of catalytic efficiency and its heterogeneity enjoyed over the reaction period. This work demonstrates the rational integration of non-noble metal catalytic sites in functionalized frameworks for the efficient fixation of CO<sub>2</sub> from dilute gas into fine chemicals.</p> <p><b>Graphical Abstract:</b> Rational construction of noble metal-free Cu(I) anchored Zr-MOF for selective capture and fixation of CO<sub>2</sub> with propargylic alcohols at atmospheric pressure conditions has been demonstrated.</p>





61.	<p><a href="#">Real-time trust aware scheduling in fog-cloud systems</a>  A Kaur, N Auluck - <i>Concurrency and Computation: Practice and Experience</i>, 2023</p> <p><b>Abstract:</b> Fog computing offers cloud-like facilities at the network edge, delivering reduced response times to latency sensitive applications. It comprises of fog devices/micro data centers/cloudlets located between users and the cloud data center. Fog devices are generally susceptible to privacy, security, and trust issues. We propose <i>RT-TADS</i> (Real Time-Trust Aware Dynamic Scheduling), a scheduling algorithm that accounts for privacy, trust and real-time performance. To compute the trustworthiness of fog devices, we propose a trust computation model. This model factors in direct and recommended trust techniques for each fog device, and updates their aggregated trust values at regular intervals. User tasks are tagged as: private, semi-private, and public. Fog devices are classified as: extremely highly trusted, highly trusted, normal trusted, low trusted, and untrusted. <i>RT-TADS</i> maps the input jobs according to their privacy constraints on trustworthy fog devices, which increases the overall Success Ratio, hence improving real-time performance. Using the Bitbrain dataset, the real-time performance of <i>RT-TADS</i> has been demonstrated, versus comparable algorithms. The results indicate that the proposed <i>RT-TADS</i> offers an average improvement of 13%, 45%, and 71% in task success ratio compared to <i>RLTCM</i>, <i>no-trust</i>, and <i>cdc-only</i> respectively.</p>
62.	<p><a href="#">Receiver for asynchronous distributed transmission over AWGN channel</a>  A Ahmad, S Agarwal - <i>National Conference on Communications</i>, 2023</p> <p><b>Abstract:</b> Distributed beamforming (DBF) paradigm allows transmission of same signal via multiple transmitters with an aim to achieve coherent reception. The key challenge in DBF is the synchronisation of various transmitters. In this paper, we focus on asynchronous transmission with an aim to detect bits from non-coherent combination of signals at the receiver and present a novel receiver framework for such a distributed asynchronous transmission. We first oversample the received signal and obtain the CFO between the transmitters. Thereafter bits are detected using the generalised likelihood ratio test. We first present the results for a single transmitter single receiver case in the presence of CFO between the two LOs and extend the same to two transmitter and a single receiver case. The performance of the two systems has been evaluated in terms of bit error rate (BER) under AWGN channel. Results show significant improvement in BER as compared with the conventional receiver.</p>
63.	<p><a href="#">Recent advances in recognition receptors for electrochemical biosensing of mycotoxins—a review</a>  M Kaur, J Gaba, K Singh, Y Bhatia, A Singh, N Singh - <i>Biosensors</i>, 2023</p> <p><b>Abstract:</b> Mycotoxins are naturally occurring toxic secondary metabolites produced by fungi in cereals and foodstuffs during the stages of cultivation and storage. Electrochemical biosensing has emerged as a rapid, efficient, and economical approach for the detection and quantification of mycotoxins in different sample media. An electrochemical biosensor consists of two main units, a recognition receptor and a signal transducer. Natural or artificial antibodies, aptamers, molecularly imprinted polymers (MIP), peptides, and DNazymes have been extensively</p>

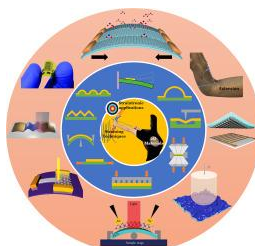
	<p>employed as selective recognition receptors for the electrochemical biosensing of mycotoxins. This article affords a detailed discussion of the recent advances and future prospects of various types of recognition receptors exploited in the electrochemical biosensing of mycotoxins.</p>
64.	<p><a href="#">Remarkably improved photocatalytic selective oxidation of toluene to benzaldehyde with O<sub>2</sub> over metal-free delaminated g-C<sub>3</sub>N<sub>4</sub> nanosheets: synergistic effect of enhanced textural properties and charge carrier separation</a>  R Ghalta, R Srivastava - <i>Catalysis Science &amp; Technology</i>, 2023</p> <p><b>Abstract:</b> The sustainable production of benzaldehyde by the oxidation of toluene with O<sub>2</sub> is a challenging and exciting research area due to the low toluene conversion over the reported catalysts and the importance of benzaldehyde in chemical industries. The photocatalytic toluene oxidation is facilitated by the generation of reactive oxygen species but is limited by charge carrier recombination. Herein a simple metal-free g-C<sub>3</sub>N<sub>4</sub> nanosheet photocatalyst is reported for the selective production of benzaldehyde by toluene oxidation with O<sub>2</sub>. The efficiency of g-C<sub>3</sub>N<sub>4</sub> was enhanced several folds just by increasing the surface area and incorporating carbon vacancies by a simple thermal treatment at different times. The best photocatalyst was obtained by thermal exfoliation at 500 °C for 3 h in a muffle furnace that exhibited 84.4% toluene conversion and ~100% benzaldehyde selectivity after 8 h using a 250 W high-pressure Hg lamp with good recyclability. The catalyst exhibited excellent activity in sunlight and produced 78.3% toluene conversion and ~100% benzaldehyde selectivity after 8 h. Toluene derivatives and other aromatic compounds were converted to their corresponding aldehydes or ketones with good yields and selectivity. The structure–activity relationship studied by catalytic investigation, physicochemical characterization, control reactions, and scavenging studies suggest that the exceptionally high surface area with carbon vacancies in exfoliated g-C<sub>3</sub>N<sub>4</sub> provides higher numbers of efficiently separated charge carriers with a longer lifetime, and facilitates the generation of various reactive oxygen species and holes responsible for the selective production of benzaldehyde with high toluene conversion and apparent quantum yield. A simple, reproducible, eco-friendly, and sustainable metal-free photocatalytic C–H activation under mild conditions would be fascinating to catalysis researchers and materials scientists to develop simple metal-free catalysts for activating other bonds with high dissociation energy to produce industrially important synthetic intermediates.</p> 
65.	<p><a href="#">Role of debridement and its biocompatibility in antimicrobial wound dressings</a>  Mohit, B Das - <i>Antimicrobial Dressings: Book Chapter</i>, 2023</p> <p><b>Abstract:</b> A wound is a breach or damage to skin tissue that results in non-functionality. Sometimes the epidermis, dermis, or muscle tissues are damaged. Skin tissue has strong self-healing abilities. However, some wounds take longer to heal or do not heal on their own, necessitating the use of an assisted healing factor. Diabetes, stroke, spinal cord injury, burns, and chronic infection are all conditions that can result in such wounds. Wound dressing is required to promote healing and protect such wounds. In general, devitalized and necrotic tissue is present at the wound site, which promotes microbial growth, inhibits wound contraction, impedes proliferation, and brings the overall wound healing cascade to a halt. Debridement is introduced in this context as a technique for removing necrotic tissue in addition to the bacterial burden present over the wound. Debridement has become a critical step in wound care. Debridement</p>

	<p>methods such as autolytic, surgical, enzymatic, mechanical, hydrosurgery, biological, and ultrasound debridement have been used for many years. Debridement in chronic wounds follows the three-dimensional principle of drainage, disruption, and division. The debridement technique should be biocompatible, simple to use, and painless. We discussed the pros and cons of the currently used tissue debridement techniques in this chapter, as well as some novel methods in the pipeline for pursuing better performing and low-risk tissue debridement.</p>
66.	<p><a href="#">Silicon carbide based nanocomposite of polythiophene with high thermally stable DC electrical conduction and ethanol sensing</a>  A Ahmad, A Husain, MA Yattoo, MMA Khan, F Habib - <i>Materials Today: Proceedings</i>, 2023</p> <p><b>Abstract:</b> Here in this work, we are reporting thermally stable DC electrical conductivity of silicon carbide nanocomposite with polythiophene and its sensing behavior towards ethanol. Polythiophene (PTh) and Polythiophene/SiC (PTh/SiC) nanocomposite were synthesized by in-situ process of polymerization via oxidation route using CTAB (cetyltrimethylammonium bromide) as a surfactant and characterized by X-rays diffraction (XRD), Fourier transforms infrared spectroscopy (FT-IR), Scanning electron microscopy (SEM) and Transmittance electron microscopy (TEM) analysis. Stability of DC electrical conductivity of PTh and PTh/SiC nanocomposite were examined at different temperature ranges from 50 °C to 130 °C in isothermal and cyclic conditions. PTh/SiC nanocomposite showed high steadiness of DC electrical conductivity than that of PTh in different thermal ageing conditions. Sensing behavior of PTh/SiC nanocomposite towards 1 M ethanol was recognized as steady with time and reversible in cyclic process.</p>
67.	<p><a href="#">Small signal stability analysis of dfig integrated power system considering pll dynamics under different grid strengths</a>  B Sahu, BP Padhy - <i>IEEE PES Conference on Innovative Smart Grid Technologies</i>, 2023</p> <p><b>Abstract:</b> The power from wind farm of DFIG technology interacts with power system through dynamics of phase-locked loop (PLL). Therefore, it is imperative to understand the participation of PLL dynamics on the power system's small signal stability (SSS). This paper focuses in investigating the interaction of PLL of a grid-connected wind farm with a multi machines power system at different grid strengths. Modal analysis is conducted on modified IEEE 39 benchmark system to study the behavior of low frequency electromechanical oscillations (LFEOS) under the influence of various conditions of grid strengths. It is revealed that, the decreasing grid strength has a remarkable impact on LFEOS, and the modes associated with PLL in such a way that they approach in the vicinity of right half of the complex plane which significantly lessens system's small signal stability. Another interesting behavior is observed that the super-synchronous operation is the riskiest state in which, even with a small active power output of wind system at weak grid condition, small signal stability reduces drastically.</p>
68.	<p><a href="#">Some algorithmic results for eternal vertex cover problem in graphs</a>  K Paul, A Pandey - <i>International Conference and Workshops: Lecture Notes in Computer Science book series</i>, 2023</p> <p><b>Abstract:</b> Eternal vertex cover problem is a variant of the vertex cover problem. It is a two player (attacker and defender) game in which given a graph <math>G=(V,E)</math>, the defender needs to allocate guards at some vertices so that the allocated vertices form a vertex cover. Attacker can attack one edge at a time and the defender needs to move the guards along the edges such that at least one guard moves through the attacked edge and the new configuration still remains a vertex cover. The attacker wins if no such move exists for the defender. The defender wins if there exists a strategy to defend the graph against infinite sequence of attacks. The minimum number of guards with which the defender can form a winning strategy is called the <i>eternal vertex cover number</i> of <math>G</math>, and is denoted by <math>evc(G)</math>. Given a graph <math>G</math>, the problem of finding the eternal</p>

	<p>vertex cover number is NP-hard for general graphs, and remains NP-hard even for bipartite graphs. We have given a polynomial time algorithm to find the Eternal vertex cover number in chain graphs and cographs. We have also given a linear-time algorithm to find the eternal vertex cover number for split graphs, an important subclass of chordal graphs.</p>
69.	<p><a href="#">Some evaluations of the Jones polynomial for certain families of weaving knots</a> S Joshi, K Negi, M Prabhakar - <i>Topology and its Applications</i>, 2023</p> <p><b>Abstract:</b> In this paper, we derive formulae for the determinant of weaving knots <math>W(3,n)</math> and <math>W(p,2)</math>. We calculate the dimension of the first <a href="#">homology group</a> with coefficients in <math>\mathbb{Z}_3</math> of the double cyclic cover of the 3-sphere <math>S^3</math> branched over <math>W(3,n)</math> and <math>W(p,2)</math> respectively. As a consequence, we obtain a lower bound of the unknotting number of <math>W(3,n)</math> for certain values of <math>n</math>.</p>
70.	<p><a href="#">Stability of a layered reactive channel flow</a> SN Maharana, KC Sahu, M Mishra - <i>Proceedings of the Royal Society A</i>, 2023</p> <p><b>Abstract:</b> We analyse the linear stability of a reactive plane Poiseuille flow, where a reactant fluid A overlies another reactant B in a layered fashion within a two-dimensional channel. Both reactants are miscible and have the same viscosity, while upon reaction, they produce either a less or more-viscous product fluid C. The reaction kinetics is of simple <math>A+B \rightarrow C</math> type, and the production of C occurs across the initial contact line of reactants A and B in a mixed zone of small and finite width. All three fluids have the same density. We demonstrate the effects of various controlling parameters such as the log-mobility ratio, Damköhler number, Schmidt number, Reynolds number, position and thicknesses of the reactive zone on the stability characteristics. We show that a tiny viscosity stratification by the reaction destabilizes the flow at a moderate (10–1000) and even at low Reynolds numbers (0.01–1). The maximum growth occurs for shorter waves than for the Tollmien–Schlichting eigenmode, and the ranges of unstable wavenumbers are wider than that known for non-reactive channel flow systems. In most cases, the instability occurs due to the overlap of the critical layer with the viscosity-stratified layer. Surprisingly for some parameters, it is observed that the reaction can make <math>\sigma M</math> decrease with increasing Reynolds number.</p>
71.	<p><a href="#">Stabilization and activation of polyoxometalate over poly(vinyl butylimidazolium) cations towards electrocatalytic water oxidation in alkaline media</a> G Singh, SD Adhikary, D Mandal - <i>Chemical Communications</i>, 2023</p> <p><b>Abstract:</b> Sandwich polyoxometalate <math>[WC_3(H_2O)_2(CoW_9O_{34})_2]^{12-}</math> (<math>Co-WC_3</math>) heterogenized with poly(vinyl butyl imidazolium) cations (<math>PVIM^+</math>) acts as a stable electrochemical water oxidation catalyst in 1 MKOH with 0.28 V @ 10 mA <math>cm^{-2}</math> overpotential and TOF of 6.16 <math>s^{-1}</math>. Various <i>in situ</i> spectroelectrochemical studies and control experiments provide the details of the catalytic activities and long-term stability of the catalyst.</p>
72.	<p><a href="#">Straining techniques for strain engineering of 2D materials towards flexible straintronic applications</a> M Pandey, C Pandey, R Ahuja, R Kumar - <i>Nano Energy</i>, 2023</p> <p><b>Abstract:</b> Straintronics of two-dimensional (2D) materials offers enormous promise for both fundamental research and smart technologies. Strain engineering of 2D materials has recently witnessed an upsurge of interest, driven by the growing demands of building flexible semiconductor devices under miniaturization. 2D materials have received considerable attention to tune their fascinating electrical, optical, and vibrational properties for flexible electronics due to their high stretchability and flexibility. For this, a variety of controllable straining techniques have been developed by mimicking either natural phenomena or mechanical processes. In the literature, strained nano-/microstructures of 2D materials have been extensively reviewed for</p>

highlighting their potential in tunable electronics, however a systematic assessment of the straining techniques utilized to create such strained structures is still lacking. In this review, we provide detailed one-to-one assessments of the straining methods used to create diverse strained structures of 2D materials and their limitations, covering recent advancements and in-depth discussions. In addition, the importance and advantages of applying straining techniques to improve the performance of flexible straintronic devices have also been covered. These will open pathways for exploiting the straining techniques for their meticulous applications.

**Graphical Abstract:**



[Structural role of osteocalcin and its modification in bone fracture](#)

S Bailey, AA Poundarik, GE Sroga, D Vashishth - *Applied Physics Reviews*, 2023

73.

**Abstract:** Osteocalcin (OC), an abundant non-collagenous protein in bone extracellular matrix, plays a vital role in both its biological and mechanical function. OC undergoes post-translational modification, such as glycation; however, it remains unknown whether glycation of OC affects bone's resistance to fracture. Here, for the first time, we demonstrate the formation of pentosidine, an advanced glycation end-product (AGE) cross-link on mouse OC analyzed by ultra-performance liquid chromatography. Next, we establish that the presence of OC in mouse bone matrix is associated with lower interlamellar separation (distance) and thicker bridges spanning the lamellae, both of which are critical for maintaining bone's structural integrity. Furthermore, to determine the impact of modification of OC by glycation on bone toughness, we glycated bone samples *in vitro* from wild-type (WT) and osteocalcin deficient ( $Oc^{-/-}$ ) mice, and compared the differences in total fluorescent AGEs and fracture toughness between the  $Oc^{-/-}$  glycated and control mouse bones and the WT glycated and control mouse bones. We determined that glycation resulted in significantly higher AGEs in WT compared to  $Oc^{-/-}$  mouse bones ( $\Delta$ -WT >  $\Delta$ -OC,  $p = 0.025$ ). This observed change corresponded to a significant decrease in fracture toughness between WT and  $Oc^{-/-}$  mice ( $\Delta$ -WT vs  $\Delta$ -OC,  $p = 0.018$ ). Thus, we propose a molecular deformation and fracture mechanics model that corroborates our experimental findings and provides evidence to support a 37%–90% loss in energy dissipation of OC due to formation of pentosidine cross-link by glycation. We anticipate that our study will aid in elucidating the effects of a major non-collagenous bone matrix protein, osteocalcin, and its modifications on bone fragility and help identify potential therapeutic targets for maintaining skeletal health.

74.

[Studies on structural changes of modified MWCNTs: material for electrochemical monitoring of antiviral drug in human serum samples](#)

R Kaur, G Bhardwaj, N Singh, N Kaur - *Chemistry – A European Journal*, 2023

**Abstract:** The development of a universal approach for precisely tuning the electrochemical characteristics of conducting carbon nanotubes for tracking harmful agents in the human body with high selectivity and sensitivity remains a challenge. Herein, we describe a simplistic, versatile, and general approach to the construction of functionalized electrochemical material. The design of electrochemical material consists of (i) modification of multiwalled carbon nanotubes (MWCNT) with dipodal naphthyl-based dipodal urea (KR-1) through non-covalent

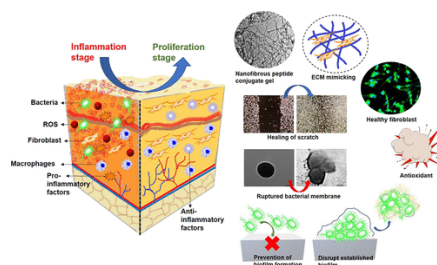
functionalization (KR-1@MWCNT) which enhances the dispersibility of MWCNT and hence conductivity, (ii) complexation of KR-1@MWCNT with Hg<sup>2+</sup> accelerate the electron transfer in the material which amplify the detection response of functionalized material (*i.e.*, **Hg/KR-1@MWCNT**) towards various thymidine analogues. Further, the application of functionalized electrochemical material (**Hg/KR-1@MWCNT**) achieves real-time electrochemical monitoring of harmful antiviral drug 5-iodo-2'-iododeoxyuridine (IUdR) levels in human serum albumin for the first time.

[Supramolecular, nanostructured assembly of antioxidant and antibacterial peptides conjugated to naproxen and indomethacin for the selective inhibition of cox-2, biofilm, and inflammation in chronic wounds](#)

M Halder, M Narula, Y Singh - *Bioconjugate Chemistry*, 2023

75.

**Abstract:** Chronic wounds are a major healthcare challenge around the world. The presence of bacterial biofilms, accumulation of reactive oxygen species (ROS), and persistent inflammation have been identified as rate-limiting steps in chronic wound healing. Anti-inflammatory drugs, like naproxen (Npx) and indomethacin (Ind), show poor selectivity for the COX-2 enzyme, which plays a key role in producing inflammatory responses. To address these challenges, we have developed conjugates of Npx and Ind with peptides possessing antibacterial, antibiofilm, and antioxidant properties along with enhanced selectivity for the COX-2 enzyme. We have synthesized and characterized peptide conjugates Npx-YYk, Npx-YYr, Ind-YYk, and Ind-YYr, which were self-assembled into supramolecular gels. As envisaged, the conjugates and gels showed high proteolytic stability and selectivity toward the COX-2 enzyme and potent antibacterial activities (>95% within 12 h) against Gram-positive bacteria *Staphylococcus aureus*, implicated in wound-related infections, eradication of biofilm (~80%), and radical scavenging (>90%) properties. Cell culture studies with mouse fibroblast cells (L929) and macrophage-like cells (RAW 264.7) showed that gels were cell proliferative in nature (120% viability), which resulted in faster and more efficient scratch healing. Treatment with gels led to a significant decrease in proinflammatory cytokine (TNF- $\alpha$  and IL-6) expressions and an increase in anti-inflammatory gene (IL-10) expression. The gels developed in this work show great promise as a topical agent for chronic wounds or as a coating for medical devices to prevent medical-device-associated infections.



[Sustainability analysis of new hybrid cooling/lubrication strategies during machining Ti6Al4V and Inconel 718 alloys](#)

N Khanna, J Airao, G Kshitij, CK Nirala, H Hegab - *Sustainable Materials and Technologies*, 2023

76.

**Abstract:** The necessity of achieving sustainable manufacturing processes, taking into account the economic and environmental balance, is a significant obstacle for many industries. This article investigates the comparative sustainability assessment of two difficult to cut superalloys (Ti6Al4V and Inconel 718) using a new hybrid sustainable machining strategy that combines ultrasonically assisted turning (UAT) with an environmentally friendly cooling and lubrication method (MQL and LCO<sub>2</sub>). The primary objective of this study is to examine the effects of the proposed strategy on the economic and carbon emission analysis, tool life, energy

	<p>consumption, and surface roughness of Inconel 718 and Ti6Al4V alloys during machining. To evaluate the efficacy of the proposed strategy for the two alloys, an in-house UAT setup is used to conduct experiments employing a variety of cooling methods. It was found that Ti6Al4V emits roughly 40% less carbon than Inconel 718. The cost of machining Ti6Al4V and Inconel 718 in a cryogenic environment decreased by about 26% and 21%, compared to a dry environment. Moreover, while machining Ti6Al4V, more tool life has improved approximately by 6–65% and 9–35% compared to Inconel 718 in CT and UAT. Machining of Ti6Al4V consumes approximately 2–16% and 9–15% less energy compared to Inconel 718 under CT and UAT, respectively. Ti6Al4V lowers the surface roughness approximately by 21% and 15% compared to Inconel 718 when using CT and UAT, respectively.</p>
77.	<p><a href="#">Synchrophasor measurement assisted control framework for voltage rise mitigation in active distribution networks</a>  K Chauhan, M Pandit, R Sodhi, HD Nguyen - IEEE 10th Power India International Conference (PIICON), 2023</p> <p><b>Abstract:</b> The active distribution networks (ADNs) are facing voltage rise (VR) issues due to massive deployment of distributed generations (DGs). To combat the VR issues, a simple yet effective voltage control framework is required which ensures a network-wide optimal control solution while taking into consideration the important parameters like measurement uncertainties, DG location's effect and DG reactive power support. To this end, a novel two-stage Synchrophasor Measurement assisted Control Framework (SMCF) is proposed in this paper. Stage-1 detects the real-time status of the voltage rise issues in the network. Upon detection of the VR problem, Stage-2 exploits the output of Stage-1 to compute two novel indices viz., locational opportunity cost (LOC) and locational reactive-power support (LQS), and formulates a multi-objective optimization problem. The proposed control framework thus provides optimal active and reactive power dispatch points for the DGs, which mitigates the VR problem from the network while ensuring minimization of active power curtailment of the DGs and maximum participation of the DGs in reactive power support. A rigorous testing reveals that the proposed method maximizes the DG revenues, mitigates voltage rise and enhances the DG hosting capacity of the network. The superiority of the proposed method has also been demonstrated in contrast to the various variants of supervisory control and data acquisition (SCADA) measurement, advanced metering infrastructure and recent synchrophasor measurement-assisted control frameworks.</p>
78.	<p><a href="#">Synergistic effect of transition metals substitution on the catalytic activity of <math>\text{LaNi}_{0.5}\text{M}_{0.5}\text{O}_3</math> (M = Co, Cu, and Fe) perovskite catalyst for steam reforming of simulated bio-oil for green hydrogen production</a>  PP Singh, A Jaswal, N Nirmalkar, T Mondal - Renewable Energy, 2023</p> <p><b>Abstract:</b> Hydrogen is considered an excellent source of renewable and sustainable energy which can be produced from inexpensive starting materials such as biomass. The present study aims at developing a stable catalytic system for bio-oil steam reforming process to produce green hydrogen. The perovskite catalysts <math>\text{LaNi}_{0.5}\text{M}_{0.5}\text{O}_3</math> (M = Co, Cu, and Fe) were synthesized using sol-gel method and their catalytic performance towards hydrogen production and bio-oil conversion was evaluated in a fixed bed tubular reactor. A wide array of techniques such as XRD, BET, <math>\text{NH}_3</math> and <math>\text{CO}_2</math>-TPD, FE-SEM, XPS, TGA and pyridine-FTIR were used to analyze the material properties of the synthesized catalysts. The results of these analyses verified the successful formation of the highly sought-after perovskite structure with good amount of surface oxygen vacancies as well as medium-strength acidic and basic sites. To establish an efficient catalytic system, process parameter (space-time and reaction temperature) optimization and time on stream (TOS) studies were conducted. The TOS results displayed that <math>\text{LaNi}_{0.5}\text{Co}_{0.5}\text{O}_3</math> perovskite catalyst is stable up to 12 h at 700 °C for space-time of 17.4 <math>\text{kg}_{\text{cat}}\cdot\text{h}/\text{kgmol}_{\text{bio-oil}}</math>. In-depth characterizations (FE-SEM, TGA, RAMAN spectroscopy and XRD) of</p>

	<p>spent catalyst after the reaction not only gave further insights about the excellent activity exhibited by the chosen catalyst but also revealed information about the nature of the coke deposited on the surface.</p>
79.	<p><a href="#">Synthesis and characterization of two potential impurities (des-ethyl-Ganirelix) generated in the Ganirelix manufacturing process</a>  S Chatterjee, A Bandyopadhyay - Journal of peptide science, 2023</p> <p><b>Abstract:</b> Controlling certain diseases using peptide drugs has remarkably increased in the past two decades. In this regard, a generic formulation is an upfront solution to fulfil market demands. Ganirelix, a leading peptide active pharmaceutical ingredient (API) primarily used as a gonadotropin-releasing hormone antagonist (GnRH), has established a potential market value worldwide. But its generic formulation mandates detailed impurity profiles from a synthetic source and contemplates the sameness of a reference-listed drug (RLD). Post-chemical synthesis and processing of Ganirelix, some commercial sources have revealed two new potential impurities among many known, which show the deletion of an ethyl group from the hArg (Et)<sub>2</sub> residue at the 6th and 8th positions, named des-ethyl-Ganirelix. These impurities are unprecedented in traditional peptide chemistry, and such monoethylated-hArg building blocks are not easily accessible commercially to synthesize these two impurities. Here, we have outlined the synthesis, purification, and enantiomeric purity characterization of the amino acids and their incorporation in the Ganirelix peptide sequence to synthesize these potential peptide impurities. This methodology will enable the convenient synthesis of side-chain substituted Arg and hArg derivatives in peptide-drug discovery platforms.</p>
80.	<p><a href="#">Techniques for the detection and management of freezing of gait in Parkinson's disease – A systematic review and future perspectives</a>  SK Bansal, B Basumatary, R Bansal, AK Sahani – MethodsX, 2023</p> <p><b>Abstract:</b> Freezing of Gait (FoG) is one of the most critical debilitating motor symptoms of advanced Parkinson's disease (PD) with a higher rate of occurrence in aged people. PD affects the cardinal motor functioning and leads to non-motor symptoms, including cognitive and neurobehavioral abnormalities, autonomic dysfunctions and sleep disorders. Since its pathogenesis is complex and unclear yet, this paper targets the studies done on the pathophysiology and epidemiology of FoG in PD. Gait disorder and cardinal features vary from festination (involuntary hurrying in walking) to freezing of gait (breakdown of repetitive movement of steps despite the intention to walk) in patients. Hence, it is difficult to assess the FoG in clinical trials. Therefore, the current research emphasizes wearable sensor-based systems over pharmacology and surgical methods.</p> <ul style="list-style-type: none"> <li>• This paper presents a technological review of various techniques used for the assessment of FoG with a comprehensive comparison.</li> <li>• Researchers are aiming at the development of wireless sensor-based assistive devices to (a) predict the FoG episode in a different environment, (b) acquire the long-term data for real-time analysis, and (c) cue the FoG patients.</li> <li>• We summarize the work done till now and future research directions needed for a suitable cueing mechanism to overcome FoG.</li> </ul> <p><b>Graphical Abstract:</b></p>



81.	<p><a href="#">Thermal stability and decomposition mechanisms of hexatetracarbon: Tight-binding molecular dynamics and density functional theory study</a>  Y Bauetdinov, A Grekova, R Sangwan - <i>Modern Physics Letters B</i>, 2023</p> <p><b>Abstract:</b> In this work, we carry out molecular dynamics and <i>ab initio</i> modeling to determine the thermal decomposition channels and thermal stability of the recently proposed 2D carbon allotrope, hexatetracarbon (HTC). To take into account the role of edges in the initialization of decay, we considered finite size cluster models of HTC passivated by hydrogen. Four models were selected for the study: <math>C_{12}H_{12}C_{12}H_{12}</math>, <math>C_{20}H_{16}</math>, <math>C_{20}H_{16}</math>, <math>C_{26}H_{18}C_{26}H_{18}</math> and <math>C_{48}H_{24}C_{48}H_{24}</math>. Molecular dynamics and hyperdynamics was carried out using the NTBM non-orthogonal tight-binding model. For <i>ab initio</i> calculations, we used the electron density functional theory with the B3LYP three-parameter hybrid functional and the 6-311G** electronic basis set. Prismane <math>C_{12}H_{12}C_{12}H_{12}</math> demonstrated the highest stability due to the high energy barrier of 1.5 eV preserving its decomposition. Larger clusters possessed lower barriers in the 0.65–0.9 eV range. We concluded that the HTC edges are unstable at room temperatures. However, the destruction of some interlayer bonds can result in strain relaxation and increase of stability. We believe that HTC could exist at room temperatures in the form of nanosized quantum dots that appeared from bilayer graphene under high pressure.</p>
82.	<p><a href="#">Towards ordered Si surface nanostructuring: role of an intermittent ion beam irradiation approach</a>  Rakhi, J Muñoz-García, R Cuerno, S Sarkar - <i>Physica Scripta</i>, 2023</p> <p><b>Abstract:</b> The dynamical characteristics of surface nanopatterning using low-energy ion beams remains a central theme within ion beam sputtering. Most previous studies have focused on nanostructure evolution by bombarding surfaces using a continuous ion beam. Here, we study the effect of sputtering from an intermittent ion beam on nanopatterning of a Si surface, using a 900 eV or (mostly) 500 eV <math>Ar^+</math> ion beam at an incident angle of <math>67^\circ</math>, up to a total fluence of <math>10 \times 10^{19}</math> ions <math>cm^{-2}</math>. Nanoripples are predominantly found on the irradiated surfaces, alongside a hierarchical triangular morphology at the lower energy condition. Ripple ordering is superior for intermediate values of the sputtering interval used in the intermittent sputtering approach. The area of the triangular structures also depends on the intermittent sputtering time intervals. At larger length scales than the ripple wavelength or the triangular structures, all surfaces display strong height fluctuations with a well-defined roughness exponent. Our results can be rationalized via known properties of the nonlinear regime of evolution for surfaces that become amorphous under irradiation and relax stress via ion-induced viscous flow, as borne out from numerical simulations of a continuum model previously proven to provide a significant description of the present class of experiments.</p>
83.	<p><a href="#">Transient over voltages in cross-bonded power cables due to lightning impulse</a>  AP Pandey, A Das, CC Reddy - <i>IEEE 10th Power India International Conference (PIICON)</i>, 2023</p> <p><b>Abstract:</b> A cable in its lifespan undergoes different transient phenomena, especially lightning. The impact of the lightning impulse was greater on the section near the termination which</p>

	<p>connects the transmission line and cable. The impact of lightning on the sheath was performed in this study using a circuit analysis for a cable with cross bonded. A simulation study presents the profile of transient voltage buildup in the sheath of a three-phase 220 kV underground power cable along the length of the cable. Since large induced voltage in the sheath may cause serious problems like an increase in the circulating current which in turn produces excessive heat that may start the melting process of the sheath and it may damage the jacket of the cable also. Due to high voltage stress between the conductor and sheath of the underground power cable, it may prematurely damage the main insulation and may lead to the failure of the power cable. The main objective of the paper is to study the transient voltage induced in the sheath of a three-phase cross-bonded underground power cable due to the lightning surge effect in the main conductor.</p>
84.	<p><a href="#">Unveiling the local structure of the amorphous metal <math>Fe_{(1-x)}Zr_x</math> combining first-principles-based simulations and modelling of EXAFS spectra</a>  G Muscas, R Johansson, S George, M Ahlberg...R Ahuja... - Scientific Reports, 2023</p> <p><b>Abstract:</b> Amorphous alloys exhibit useful properties such as the excellent soft magnetic behaviour of Fe-based metallic glasses. The detailed structure of amorphous <math>Fe_{(1-x)}Zr_x</math> with <math>x = 0.07, 0.10, \text{ and } 0.20</math> is in this work explored through a synergetic combination of atomistic simulations and experimental characterisation. Thin-film samples were investigated using X-ray diffraction and extended X-ray absorption fine structure (EXAFS), while the corresponding atomic structures were simulated using an efficient first-principles-based method called stochastic quenching (SQ). The simulated local atomic arrangements are investigated by constructing the radial- and angular-distribution functions, as well as by Voronoi tessellation. The radial distribution functions are then used to construct a model to fit simultaneously the experimental EXAFS data of multiple samples with different compositions, creating a simple yet accurate description of the atomic structures valid for any composition in the range <math>x = 0.07</math> to <math>0.20</math>, using a minimal number of free parameters. This approach significantly improves the accuracy of the fitted parameters and allows us to relate the compositional dependence of the amorphous structures with the magnetic properties. The proposed EXAFS fitting process can be generalised to other amorphous systems, contributing to the understanding of structure-property relationships and the development of amorphous alloys with tailored functional properties.</p>
85.	<p><a href="#">Willingness to pay and its determinants for improved solid waste management: a case study</a>  M Ray, PK Ryngnga, P Chetia - International Journal of Environment and Waste Management, 2023</p> <p><b>Abstract:</b> This study aimed to find out the probability of willingness to pay for an improved system to manage solid wastes generated in an Indian municipality using the contingent valuation method. To determine the socio-economic factors that affect the probability of willingness to pay, binary logistic regression was applied. Most of the residents are willing to pay extra money in form of direct donation or tax to get better waste management facilities and services. Although it is found that year of effective schooling, income, awareness of Swachh Bharat Abhiyan, and distance of community bin from households have positive and statistically significant effect on residents' willingness to pay, while gender played a negative and significant role in determining willingness to pay. The findings of this study could contribute to design a more sustainable system for residential waste management.</p>

**Disclaimer:** This publication digest may not contain all the papers published. Library has compiled the publication data as per the alerts received from Scopus and Google Scholar for the affiliation “Indian Institute of Technology Ropar” for the month of March 2023. The author(s) are requested to share their missing paper(s) details if any, for the inclusion in the next publication digest.